

Pasting and gelation of faba bean starch-protein mixtures

Klara Nilsson^{a,*,1}, Mathias Johansson^{a,*,1}, Corine Sandström^a, Hanna Eriksson Röhnisch^a, Mikael S. Hedenqvist^b, Maud Langton^a

^a Department of Molecular Sciences, Swedish University of Agricultural Sciences, Box 7015, SE-750 07, Uppsala, Sweden

^b Division of Polymeric Materials, Department of Fibre and Polymer Technology, KTH-Royal Institute of Technology, 10044, Stockholm, Sweden

ARTICLE INFO

Keywords:

Faba bean
Protein
Starch
Texture
Microstructure
Gelation

ABSTRACT

Starch and protein are major components in many foods, contributing to nutritional and textural properties. Understanding how the behaviour and interactions of these components contribute to different textures is important. In this study, mixed gel systems were created with different ratios of starch to protein (constant solid content 12%) extracted from faba bean, a promising crop for locally produced plant-based foods in cold climate regions. The mixed starch-protein gels were characterised in terms of pasting, texture and microstructure. Starch-rich mixtures showed higher water binding and water absorption than samples with higher protein content. A tendency for more efficient hydration in starch-rich samples was confirmed by NMR. Iodine affinity appeared to be lower for high-protein samples, particularly at higher temperatures. Mixtures with high starch content also showed higher viscosity during pasting, higher storage modulus throughout gelation, lower $\tan \delta$ and lower frequency dependence of the final gel. Characterisation by compression tests showed stronger and more elastic gels with increasing starch content. Light microscopy revealed that starch granules were tightly packed, especially at higher starch content, with protein filling the spaces between starch granules. SEM micrographs revealed a network structure with larger pores and thicker strands in samples with higher starch content. Overall, increasing protein content reduced viscosity during pasting and caused softer gels, likely owing to different gelation and hydration properties of starch and protein.

1. Introduction

Transitioning to more plant-based diets is suggested to have nutritional and environmental benefits (Rööös et al., 2020; Willett et al., 2019). Across Europe, a trend for greater interest in plant-based foods is emerging (Aschemann-Witzel, Gantriis, & Fraga, 2021). There are many reasons why consumers opt for plant-based foods, including health, sustainability and animal welfare (Aschemann-Witzel et al., 2021). Consumers are now demanding a greater array of plant-based products using simple ingredients with good organoleptic properties. Faba bean already has an established market for animal feed and an emerging market for human consumption, and is a high-protein crop that can be grown in Northern Europe. With increased research and technological innovation, faba bean has the potential to be used in locally produced and sustainable plant-based foods (Multari, Stewart, & Russell, 2015).

Under appropriate processing conditions, faba bean starch and faba

bean protein can both act as a gelling agent, but with different gelling abilities and properties. In real food matrices, starch and protein are likely to be blended and interactions between the biopolymers will influence the formation and texture of the final gel. Depending on the final food product, different gel textures and structures will be acceptable. The gelling properties and mixability of starch and protein are among the most important features in food formulation (Onwulata, Tunick, & Thomas-Gahring, 2014; Schorsch, Wilkins, Jones, & Norton, 2001).

Gelatinisation is a process whereby starch granules swell and leach out amylose during heating in excess water. According to Walstra (2002), as the system cools a gel can develop through the formation of microcrystallites between the amylose chains and/or as a closely packed system of granules, with the amylose layer acting as glue between the granules. Faba bean starch gels are reported to be strong and firm (Li et al., 2019). Faba bean also has high final viscosity during pasting, which has been attributed to the relatively high amylose content

* Corresponding author.

** Corresponding author.

E-mail addresses: klara.nilsson@slu.se (K. Nilsson), mathias.johansson@slu.se (M. Johansson).

¹ These authors contributed equally.

(Ambigaipalan et al., 2011; Li et al., 2019; Punia, Dhull, Sandhu, & Kaur, 2019; Zhang, Tian, Wang, Jiang, & Li, 2019) that aggregates to form a gel network upon cooling. High amylose content has also been related to retarded swelling of starch granules (Nilsson et al., 2022; Sasaki & Matsuki, 1998; Tester & Morrison, 1990; Vamadevan & Bertoft, 2020). Faba bean starch has been found to leach out more amylose than other bean varieties with similar amylose content, contributing to a rise in viscosity (Ambigaipalan et al., 2011; Ambigaipalan, Hoover, Donner, & Liu, 2013). Two other factors that result in faba bean starch gels having higher viscosity than e.g. wheat starch gels are larger size of the swollen granules and higher prevalence of larger polymer chains (Nilsson et al., 2022). Amylose and amylopectin molecular weight in faba bean starch is reported to be 10–20 MDa and 60–100 MDa, respectively, and heating the starch at a higher rate (12 °C/min vs 1.5 °C/min) to temperatures below peak viscosity (119 °C for faba bean) has been found to produce the most viscous gels (Nilsson et al., 2022). The temperature range for gelatinisation of faba bean starch has been shown to be 59–75 °C (Ambigaipalan et al., 2011; Li et al., 2019; Nilsson et al., 2022; Punia et al., 2019; Zhang et al., 2019), with pasting commencing at around 77 °C.

Similarly to starch gelatinisation, protein gelation is an essential process in the production of many foods. Most legumes, including faba bean, contain mainly globular proteins (Kimura et al., 2008; Nicolai & Chassenieux, 2019). The globular proteins in faba bean can be divided into two major fractions, hexameric legumin-type (11S) and trimeric vicilin-type (7S) globulins, with an approximate size of 330 and 150 kDa, respectively (Sharan et al., 2021; Warsame, O'Sullivan, & Tosi, 2018). Gelation of globular proteins occurs by complete or partial denaturation of the protein, exposing hydrophobic residues and other interaction sites (Zha, Rao, & Chen, 2021). The newly exposed parts of the protein interact and aggregate to form a network if the protein concentration is sufficiently high (Zha et al., 2021). The gelation process and gel properties of proteins are affected by multiple factors, such as pH, presence of salt, extraction method and protein source (Langton et al., 2020; Ma et al., 2022; Nicolai & Chassenieux, 2019). A denaturation point within the range 75–95 °C, depending on the ionic strength of the environment, has been reported for the 7S and 11S fractions in faba bean protein (Kimura et al., 2008). Gelation of faba bean protein and the effects of salt, pH and extraction method have been studied previously (Langton et al., 2020). The effect of partly replacing faba bean protein with starch and/or fibre has been investigated previously, resulting in an increased storage modulus of gels whilst the fracture stress was simultaneously reduced (Johansson, Johansson, et al., 2022).

In brief, concentrated starch gels can be described as a composite system consisting of swollen granules embedded in a three-dimensional network of aggregated amylose chains (Yang, Irudayaraj, Otgonchimeg, & Walsh, 2004), while globular proteins form fine-stranded gel networks at high repulsion or a coarse-stranded network of colloidal particles as the isoelectric point is approached (Langton et al., 2020; Langton & Hermansson, 1992). Depending on the ratio of starch to protein, gel formation and properties may differ, with e.g. higher protein content in starch-protein composite gels being associated with augmented pasting temperature and reduced gel firmness (Bravo-Núñez, Garzón, Rosell, & Gómez, 2019; Joshi, Aldred, Panozzo, Kasapis, & Adhikari, 2014; Núñez-Santiago, Bello-Pérez, & Tecante, 2004; Oñate Narciso & Brennan, 2018; Onwulata et al., 2014; Ribotta, Colombo, León, & Añón, 2007; Yang et al., 2004). According to Eliasson (1983), higher protein content alters the water retention capacity of the system because the proteins compete with starch for available water, thereby causing an increase in pasting temperature. Protein adsorption to granule surfaces during pasting could explain both the reduced pasting viscosity and increased pasting temperature, as the adsorbed proteins would restrict water diffusion and thus reduce and delay granule swelling (Bravo-Núñez et al., 2019; Bravo-Núñez & Gómez, 2019; Oñate Narciso & Brennan, 2018). Joshi et al. (2014) found that the pasting temperature increased from 73.5 °C in 100% starch systems to 82.4 °C in

50:50 lentil starch/lentil protein systems, and attributed this to the characteristically high denaturation temperature (118 °C) of lentil protein isolate. The decrease in pasting viscosity with increasing protein content may also be partly due to an overall reduction in the starch fraction, as starch tends to form more viscous pastes. However, the apparent viscosities of blends were reported to be higher in the corresponding diluted starch systems, indicating that protein-starch interactions also alter the gelatinisation and gelling properties (Bravo-Núñez et al., 2019; Bravo-Núñez & Gómez, 2019).

Breakdown viscosity has also been found to be lower for starch-protein mixtures compared to that of the corresponding sample containing only starch (Oñate Narciso & Brennan, 2018; Onwulata et al., 2014). In a study adding 10% extra protein, breakdown of starch-protein mixed pastes was no longer detected, suggesting that the protein gel network increased the resistance to mechanical shearing (Joshi et al., 2014). During cooling of starch dispersions, gelation occurs as amylose and amylopectin aggregate to form a gel network, but higher protein content has been found to correlate with a reduction in final viscosity (Bravo-Núñez et al., 2019; Bravo-Núñez & Gómez, 2019; Joshi et al., 2014; Oñate Narciso & Brennan, 2018; Onwulata et al., 2014; Ribotta et al., 2007). The amylose:amylopectin ratio in starch has been shown to have an effect on the viscosity and gel strength of composite gels, with the reduced viscosities associated with incorporation of protein being more pronounced for high-amylose starches (Joshi et al., 2014; Oñate Narciso & Brennan, 2018). Studies by Oñate Narciso and Brennan (2018) and Onwulata et al. (2014) revealed that proteins appeared to prevent molecular rearrangement of amylose, resulting in weaker gels. In contrast, the rigidity of high-amylopectin starch gel has been shown to increase with additional protein, as the protein acts as a filler (Onwulata et al., 2014).

Gels with higher solids content tend to be firmer and stronger, e.g. Yang et al. (2004) found that the reducing effect of protein on gel firmness became less marked as the solids content increased. Shim and Mulvaney (2001) observed a similar effect in gels with 15% solids content, where addition of whey protein isolate had a diluting effect on corn starch (Shim & Mulvaney, 2001). As the solids content increased to 30% in that study, separate phases in the mixtures were still present but the complex modulus (G^*) increased, suggesting that the gel structure was maintained by the higher solids content.

The aim of the present study was to evaluate gel formation and pasting properties of different faba bean starch-protein gel mixtures. Gel microstructures were evaluated and continuous and discrete phases in the gels were identified. The gel structures observed were then compared against physical and textural attributes of the gels. By understanding the role of protein and starch in composite gel systems, products with tailored textures and functionality can be developed.

2. Materials and methods

To assess gel formation and properties, different analytical techniques were applied at different stages of gel production. The key steps in gel production are summarised, together with the analytical techniques applied during the different steps of gel formation, in Fig. S1 in Supplementary Information (SI).

2.1. Materials

The protein and starch fractions used in this study were isolated from dehulled and finely milled faba beans (*Vicia faba* var. Gloria) grown in central Sweden, harvested and dried in 2016. The beans were kindly provided by RISE (Research Institutes of Sweden). Based on previous characterisations by Johansson, Johansson, et al. (2022), the composition of the protein fraction was: protein 77.3%, starch 0.3%, fibre 1.0%, fat 3.4% and ash 8%, while that of the starch fraction was: protein 0.5%, starch 94.5%, fibre 2.2%, fat 0.3% and ash 0.2%.

Hydrochloric acid (HCl) and sodium hydroxide (NaOH) were

purchased from Merck, ethanol from Solveco, osmium tetroxide and glutaraldehyde from Ted Pella, ruthenium red and light green from Sigma-Aldrich, Technovit 7100 from Kulzer and iodine from Fluka.

2.2. Extraction

Extraction of the protein and starch fractions was performed using methodology described previously (Johansson, Nilsson, Knab, & Langton, 2022). In brief, dehulled and milled faba beans were dispersed in de-ionised water with pH adjusted to 9. Protein was separated from starch and fibre by centrifugation and precipitated from the supernatant by adjusting the pH to 4. The mixture was further centrifuged and washed once before adjusting the pH back to 7 and freeze-drying. The pellet from the initial centrifugation was used to extract starch. First, the pellet was re-dispersed in de-ionised water and the pH was adjusted to 9.5. The mixture was then stirred for 24 h at room temperature and left to stand without agitation for an additional 24 h at 4 °C, followed by centrifugation and washing until pH 7 was reached. Finally, the starch was separated by filtering through a 70 µm nylon filter and dried at 40 °C.

2.3. Gel formation

Starch and protein flours were mixed well and then dispersed in distilled water to obtain a final concentration of 12% (g flour/g sample). The following starch:protein (S:P) ratios were produced (values in brackets are percentage starch or protein in the total sample):

S100P0: Starch 100% (12%), protein 0% (0%)
 S90P10: Starch 90% (10.8%), protein 10% (1.2%)
 S80P20: Starch 80% (9.6%), protein 20% (2.4%)
 S70P30: Starch 70% (8.4%), protein 30% (3.6%)
 S60P40: Starch 60% (7.2%), protein 40% (4.8%)
 S0P100: Starch 0% (0%), protein 100% (12%)

Initial trials conducted to identify the ideal solids content for the gels revealed that 12% solids content was a good intermediate concentration, as S60P40 samples were able to form freestanding gels and S90P10 samples did not form too viscous pastes for handling during the gel-making process.

To make the gels, the dispersions were stirred at 500 rpm at room temperature for 40 min and then stirred in a water bath at 65 °C for an additional 20 min, with the aim of avoiding sedimentation of the starch and maintaining a homogenous mixture for gelation. To produce gels of suitable size for compression tests and microscopy, 3-mL samples were loaded into hollow glass tubes with inner diameter 12 mm. The bottom of each glass tube was closed with a rubber lid and the top with thread tape punctured with a small hole to prevent pressure build-up. The samples were heated in a water bath (DYNEO DD-1000F Refrigerated/heating circulator, Julabo, Seelbach, Germany) from 65 to 95 °C at a rate of 1.5 °C/min. After a 30-min holding time at 95 °C, the samples were cooled to 25 °C at a rate of 1.5 °C/min. The gels were then left at room temperature for approximately 30 min before being stored at 4 °C overnight.

2.4. Hydration and water binding properties by centrifugation

Hydration and water binding properties were analysed before and after heat treatment, following the methodology of Bravo-Núñez and Gómez (2019) with some slight modifications. The hydration properties were assessed by measuring water binding capacity (WBC), i.e. the amount of water retained by samples before heating, which was determined by making 12% (w/v) flour mixture-water solutions. To ensure complete dispersion, the samples were quickly vortexed before being magnetically stirred for 40 min at 500 rpm. The samples were then centrifuged at 580×g for 10 min, the excess water was removed and the

remaining hydrated solids were weighed. WBC was calculated as grams of water retained per gram of dry sample.

For further assessment of the water binding properties after heat treatment, water absorption index (WAI), swelling power (SP) and water solubility index (WSI) were determined (Bravo-Núñez & Gómez, 2019). For analysis, 120 mg of sample (W_i) were dispersed in 1 mL of de-ionised water and the samples were prepared in the same manner as described in section 2.3 until cooling to 25 °C. The samples were then left to stand overnight at 4 °C, prior to being centrifuged at 3000×g at 4 °C for 10 min. The supernatant was decanted and dried at 105 °C for 8 h, giving the dry solids weight (W_s). The remaining pellet was also weighed (W_r). WAI, WSI and SP were calculated using the following equations:

$$\text{Water Absorption Index} \left(\frac{\text{g}}{\text{g}} \right) = \frac{W_r}{W_i} \quad (1)$$

$$\text{Water Solubility Index} \left(\frac{\text{g}}{100\text{g}} \right) = \frac{W_s}{W_i} * 100 \quad (2)$$

$$\text{Swelling Power} \left(\frac{\text{g}}{\text{g}} \right) = \frac{W_r}{W_i - W_s} \quad (3)$$

2.5. NMR spectroscopy

Sample preparation for nuclear magnetic resonance (NMR) spectroscopy followed the method described by Larsen et al. (2013) with slight modification. For this, 50 µg of flour or flour mixtures with starch:protein ratio 60:40 and 90:10 were weighed out and packed into 4 mm ZrO₂ rotors. The moisture content in the flours was 4.0% (starch) and 6.4% (protein). Then 50 µL of D₂O were inserted into the rotor using a Hamilton Microliter® #810 syringe. To equilibrate the D₂O within the rotor, the samples were left to stand for 1 h prior to spinning at 9 kHz for 1 h to ensure proper mixing of flour and D₂O.

NMR spectra (carbon-13 (¹³C) cross-polarisation magic angle spinning (CPMAS) and single-pulse excitation magic angle spinning (SPMAS) were obtained using a Bruker Avance III 600 MHz spectrometer equipped with a double-resonance 4 mm (1H&19F)/(15N-31P) CPMAS probe. The CPMAS spectra were recorded with a contact time of 1–2 ms and a repetition delay of 2.5–5 s. The NMR measurements were performed at a spinning frequency of 8 kHz and at three different temperatures; first at 25 °C before heating, then at 85 °C and finally at 25 °C after cooling. The maximum temperature was set to 85 °C, due to the limits of the instrument. All samples were analysed in triplicate.

2.6. Hot-stage microscopy

Swelling of the starch granules was visualised following the method described by Nilsson et al. (2022). Suspensions with starch-protein mixtures of 10 mg/mL were mixed for 40 min and then 80 µL of sample were pipetted onto a cover slip and 15 µL of diluted Lugol's stock solution were added to dye the starch. The samples were covered with a slightly smaller coverslip and sealed using nail polish. A tensile strength test stage (model TST350, Linkam Scientific Instruments, Surrey, UK) with heating capacity was attached to the light microscope (Nikon Eclipse Ni-U microscope, Tokyo, Japan) for temperature control. The heating rate was 5 °C/min within the range 30–95 °C. Samples were observed under bright-field light using a Plan Fluor 10 × (0.30 N.A.) objective. For observations under polarised light, samples were prepared in the same manner, with the exception of iodine staining. Micrographs were captured with a Nikon Digital Sight DS-Fi2 camera (Nikon, Tokyo, Japan) every 12 s. Captured micrographs had a pixel size of 1.21 µm (data size: 2560 × 1920 pixels). All micrographs acquired were analysed and compared visually, to pinpoint the temperature at which major changes in granules occurred.

2.7. Effect of heating on iodine dyeing of starch

To test the effect of heating on iodine dyeing, 200 mg flour were dispersed in 20 mL distilled water in capped heat-proof glass test tubes, 2 mL of Lugol's solution were added to each sample and the samples were heated in a water bath from 20 to 95 °C at 1.5 °C/min. Starting at 20 °C and at 10 °C intervals up to the final temperature (90–95 °C), the test tubes were shaken to ensure that flour and iodine were dispersed in the mixtures and 1-mL aliquots of each solution were collected in separate Eppendorf tubes and immediately placed on ice to cool. Duplicate 200 µL aliquots were then pipetted onto a 96-well plate. The samples were shaken for 2 min and absorbance was measured at 510 nm. Distilled water with iodine subjected to the same heat treatment was used as a control. All samples were analysed in duplicate.

2.8. Rheology

2.8.1. Pasting (95 °C)

Pasting data were obtained using a Discovery HR-3 rheometer (TA Instruments, New Castle, DE, USA) equipped with a Peltier pressure cell and steel starch paddle. Starch-protein mixtures with a solids content of 12% in solution were mixed at 20 °C for 40 min at the instrument maximum of 50 rad/s. For the remainder of the experiment the stirring rate was set to 16.75 rad/s, which is equivalent to the standard rotational rate of 160 rpm used in the rapid visco-analyser. As in the gelation process, samples were heated to 95 °C at a heating rate of 1.5 °C/min and kept at 95 °C for 30 min under constant stirring. Samples were cooled to 25 °C at a cooling rate of 1.5 °C/min and then kept for 30 min at 25 °C under constant stirring. All samples were analysed in duplicate.

2.8.2. High-temperature pasting (150 °C)

To investigate how the starch:protein ratio influenced peak viscosity, high-temperature pasting measurements were performed. Previous work has reported that peak viscosity of (pure) faba bean starch occurs at 119 °C (Nilsson et al., 2022). However, initial high-temperature pasting trials on the starch-protein mixtures in the present study revealed that the samples needed to be heated to 150 °C to guarantee that peak viscosity was achieved for all samples.

As in the lower-temperature pasting experiments (section 2.8.1), the flour solutions were mixed in the instrument for 40 min at 50 rad/s at 20 °C. During the pasting analysis, the heating cycle used was 20–150–25 °C with a heating and cooling rate of 5 °C/min and a constant stirring rate of 16.75 rad/s. The samples were kept for 5 min at the maximum temperature (150 °C) and 5 min at the end-set (25 °C) temperature. The main aim of the high-temperature pasting analysis was to determine how peak viscosity differed between the samples and identify any behavioural pattern present depending on the starch:protein ratio. The higher heating/cooling rate was applied to improve experimental efficiency, by reducing the time required for each trial, as overall relative pasting behaviour of the samples did not appear to change. Samples were analysed in duplicate.

2.8.3. Oscillatory rheology

The gelation process and viscoelastic properties of the gels were evaluated using a Discovery HR-3 rheometer (TA Instruments, New Castle, DE, USA) equipped with a 40-mm aluminium plate. Samples were prepared as described in section 2.3, excluding the final gelation step in the glass tubes. Paraffin oil, covering the exposed parts of the sample, was combined with a custom-made solvent trap to limit evaporation. The gelation process was monitored at 0.5% strain during a temperature ramp consisting of heating from 65 °C to 95 °C at a rate of 1.5 °C/min and 30 min holding time at 95 °C before cooling at 1.5 °C/min to 25 °C, followed by an additional holding time of 30 min. After the temperature ramp, a frequency sweep was run from 0.628 to 100 rad/s at 0.5% strain and 25 °C. Finally, an amplitude sweep was performed from 0.01 to 100% at 1 Hz and 25 °C to determine the linear viscoelastic

region (LVR) and ensure that all measurements were performed within this region. The LVR was defined as the strain at which a 5% loss in storage modulus was observed. All oscillatory rheology measurements were performed in triplicate.

2.9. Compression tests

Gels prepared as described in section 2.3 were allowed to equilibrate to room temperature for 1 h before being cut into cylindrical pieces with height 14 mm and diameter 12 mm. The samples were compressed to 70% of their original height at a rate of 1 mm/s using a texture analyser (Stable Micro Systems, TA-HDi, Surrey, UK) equipped with a 500 N load cell and a 36 mm cylindrical aluminium probe. A trigger force of 0.05 N was used to initiate measurement and data collection. Due to the weak nature of the 60:40 gels, a trigger force of 0.01 N was used to reduce the compression of these gels occurring before data collection started. To account for changes in cross-section during compression, true stress and true strain were calculated as described previously (Munialo, van der Linden, & de Jongh, 2014). True fracture stress and true fracture strain (hereafter referred to simply as fracture stress and fracture strain) were defined as the maximum true stress and corresponding true strain at the first clear peak before fracture. Young's modulus was calculated as the slope of the true stress-true strain curve during the initial 1–5% of deformation. This specific region (1–5%) was chosen to be within the initial linear region of the curve without including the potentially noisy first few measurements. Compression tests were performed for each sample, in three batches of 4–8 gels each. Statistical analysis was performed on the mean value obtained for each batch.

2.10. Microstructural characterisation of gels

Gels for microscopy were prepared as described in section 2.3. Samples for both light microscopy and scanning electron microscopy (SEM) were prepared similarly as described previously (Johansson, Johansson, et al., 2022).

2.10.1. Light microscopy

Gels were cut into approximately $2 \times 2 \times 2$ mm³ cubes and fixated overnight in 2.5% glutaraldehyde and 0.1% ruthenium red. The gels were then further fixated in 1% osmium tetroxide for 2 h, followed by dehydration in a series of solutions with increasing ethanol concentration. Thereafter, the gels were embedded using Technovit 7100 and sectioned (Leica Microsystems GmbH, Leica EM UC6, Wetzlar, Germany) into 1 µm thick sections. The light microscope (Nikon, Eclipse Ni-U microscope, Tokyo, Japan) was equipped with a 60 × (1.4 N.A.) plan apochromatic objective and micrographs were captured using a Nikon Digital Sight DS-Fi2 camera (Nikon, Tokyo, Japan) with 0.08 µm/pixel (data size: 2560 × 1920 pixels).

2.10.2. Scanning electron microscopy

For SEM, samples were prepared as for light microscopy up to dehydration in ethanol. After dehydration, the samples were critical point-dried (Quorum Technologies Ltd, K850 Critical Point Dryer, East Sussex, UK), fractured and sputter-coated with gold (Cressington Scientific Instruments, Sputtercoater-108 auto, Watford, UK). Samples were then examined in the SEM device (Hitachi, FlexSEM 1000II, Tokyo, Japan) at 5 kV and micrographs were digitally recorded at two different magnifications (9.92 and 4.96 nm/pixel, data size: 2560 × 1920 pixels).

2.11. Statistical analyses

Data on hydration and water binding properties, rheological measurements and results of compression tests were analysed by analysis of variance (ANOVA) and pairwise comparison (Tukey) with a significance level of 95% ($p < 0.05$), using R studio (Version 1.2.5033, RStudio Inc., MA, USA). After evaluation of the residuals, G' , end of LVR, n -values and

fracture stress values were log-transformed to obtain normally distributed residuals before statistical analysis (ANOVA and pairwise comparison (Tukey)). Similarly, the inverse of $\tan \delta$ values was used in statistical analysis. Pearson correlation coefficients were calculated to gain an overall understanding of parameters affected by the starch:protein ratio and to determine whether correlations between the parameters were significant.

3. Results and discussion

3.1. Hydration and water binding properties

The water binding capacity (WBC) increased with increasing starch content (Table 1). A negative WBC was observed for the sample containing only protein (SOP100), presumably because the protein dissolved in the water and was decanted with the supernatant.

The water absorption index (WAI) values of all samples increased dramatically after heat treatment but the gels with higher starch content still had higher water absorption, indicating that starch had a higher affinity for water than protein. The swelling power (SP) value also increased with increasing starch content and the correlation between WAI and SP was high ($r = 0.86$; $p = 0.002$). The swelling power of starch granules has previously been found to correlate with amylopectin content and faster heating rate (Nilsson et al., 2022; Tester & Morrison, 1990).

The WSI value of the samples increased with increasing protein content. The supernatant from both the hydration and gelation analysis was much clearer for the composite mixtures with higher starch content, corresponding to lower WSI.

3.2. NMR results

The ^{13}C -CPMAS NMR spectra at 25 °C of powder of starch, protein and a 50:50 starch-protein mixture are shown in Fig. 1, with assignments of the C1 to C6 resonances of the glucose-repeating unit in the starch indicated on top of the spectra. Assignments of the major protein signals are also shown.

Hydration often leads to large changes in the molecular mobility of starch. ^{13}C solid-state NMR has been used in a number of studies to follow hydration of the polysaccharide (Garbow & Schaefer, 1991; Larsen, Blennow, & Engelsens, 2008; Larsen et al., 2013; Morgan, Furneaux, & Larsen, 1995; Tang & Hills, 2003; Zhu, 2017). Two types of ^{13}C NMR spectroscopy, CPMAS and SPMAS, were used to monitor hydration in this study. Cross-polarisation (CP) depends on heteronuclear dipolar couplings between the ^1H and ^{13}C nuclei and if these couplings are averaged because of rapid molecular motion due to hydration, then CP will not occur. NMR signals from mobile components can be observed instead by a single pulse NMR experiment as performed in the solution-state. The CPMAS signals are interpreted as “rigid” carbons and SPMAS signals as “mobile” carbons. Thus, in CPMAS spectra, resonances

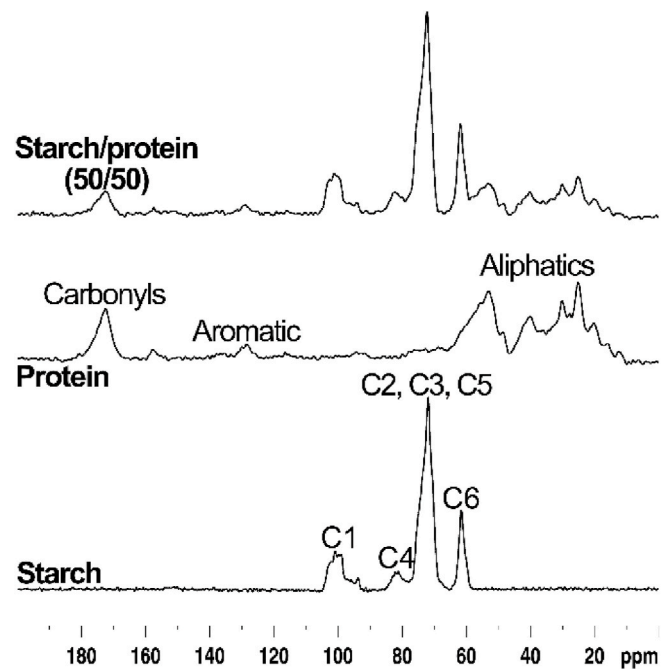


Fig. 1. Nuclear magnetic resonance ^{13}C -CPMAS spectra of powder of (top) 50:50 (w/w) starch-protein mixture, (middle) protein and (bottom) starch.

from carbons originating from immobile regions are enhanced, while in SPMAS spectra carbon resonances from immobile and mobile regions are enhanced.

Addition of water to starch resulted in attenuation of signal intensities in the amorphous region. After addition of water, the signals around 80–84 ppm, corresponding to C4, almost completely disappeared (Figs. 1 and 2). This is consistent with previous findings and derives from hydration-induced mobilisation of the amorphous starch, leading to reduced cross-polarisation efficiency. Hydration also resulted in an increase in spectral resolution for the ordered polysaccharide, due to reduced conformational distribution and substantial decreases in the signals from the amorphous region. The signals in the SPMAS spectra were sharp and the spectra were similar, although with broader resonances, to the solution-state spectra of soluble starch (Fig. 2). The increase in temperature to 85 °C led to a strong decrease in signal to noise ratio in the CPMAS spectra, but to a significant increase in spectral resolution in the SPMAS spectra. This indicates, as shown previously by others, that gelatinisation reduced the amount of immobile fraction of starch. Lowering the temperature back to 25 °C led to NMR spectra similar to those obtained before the temperature increase.

Addition of water to the S90P10 and S60P40 samples gave CPMAS and SPMAS spectra for starch that were similar to those obtained for starch alone (Figs. 2 and 3). However, closer inspection showed some small differences between the S90P10 and S60P40 samples, e.g. the C4 resonances at 80–84 ppm were not completely eliminated in the CPMAS spectra of the S60P40 samples at 25 °C. Narrower lines in the SPMAS NMR spectra are indicative of more efficient hydration and higher mobility. Thus, the narrower line width of the resonance in the SPMAS spectra of the S90P10 samples (60–90 Hz) compared with the S60P40 samples (130–140 Hz) suggests that hydration of starch was slightly more efficient in the S90P10 samples at 25 °C.

The differences between the S90P10 and S60P40 samples became more clear upon heating to 85 °C. The S90P10 samples showed results similar to that of pure starch, with a clear decrease in the signal to noise ratio in the CPMAS spectra and a significant increase in spectral resolution in the SPMAS spectra (Fig. 3). In contrast, only a slight decrease in the signal to noise ratio in the CPMAS spectra was observed for the S60P40 samples upon heating. Furthermore, the increase in spectral

Table 1

Hydration and water binding properties of the starch-protein (S%P%) mixtures. Values shown are mean \pm 1 st.dev. Different superscript letters indicate significant differences ($p < 0.05$).

	Water binding capacity (WBC)	Water absorption index (WAI)	Water solubility index (WSI)	Swelling power (SP)
S100P0	1.4 \pm 0.0 ^a	11.7 \pm 0.4 ^a	2.5 \pm 0.1 ^f	12.0 \pm 0.4 ^a
S90P10	1.2 \pm 0.0 ^b	10.3 \pm 0.2 ^b	5.7 \pm 0.4 ^e	10.9 \pm 0.2 ^b
S80P20	1.1 \pm 0.0 ^c	9.5 \pm 0.0 ^c	12.5 \pm 0.5 ^d	10.8 \pm 0.03 ^b
S70P30	0.9 \pm 0.1 ^d	8.1 \pm 0.1 ^d	20.0 \pm 0.6 ^c	10.2 \pm 0.1 ^{b,c}
S60P40	0.8 \pm 0.0 ^e	7.0 \pm 0.3 ^e	29.7 \pm 2.6 ^b	9.9 \pm 0.1 ^c
SOP100	-0.4 \pm 0.1 ^f	2.5 \pm 0.2 ^f	73.6 \pm 1.8 ^a	9.6 \pm 0.4 ^c

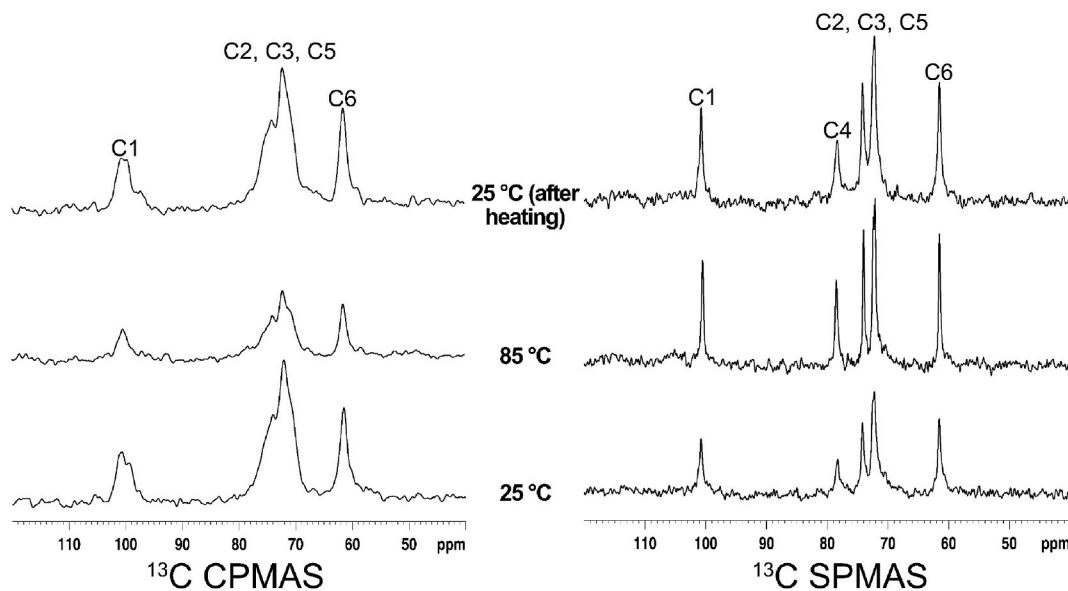


Fig. 2. Nuclear magnetic resonance ^{13}C CPMAS spectra (left) and SPMAS spectra (right) of hydrated starch (top) at 25 °C after heating to and cooling from 85 °C, (middle) at 85 °C and (bottom) at 25 °C. CPMAS signals interpreted as “rigid” carbons and SPMAS signals as “mobile” carbons.

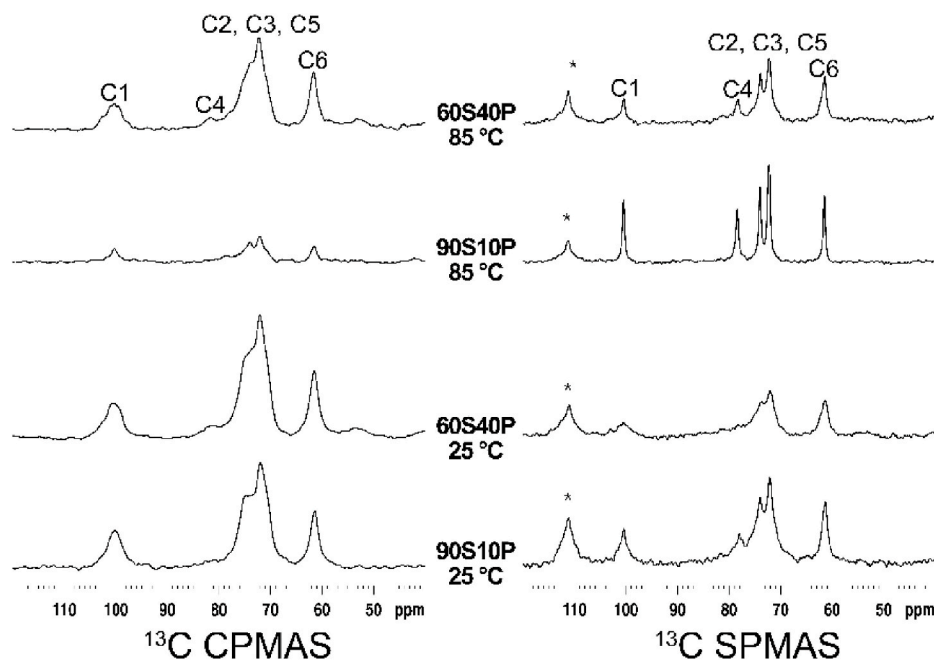


Fig. 3. Nuclear magnetic resonance ^{13}C CPMAS spectra (left) and ^{13}C SPMAS spectra (right) of (top to bottom) the samples S60P40 at 85 °C, S90P10 at 85 °C, 60S40P at 25 °C and 90S10P at 25 °C. *Background signal.

resolution was less pronounced for the S60P40 samples compared to the S90P10 samples. This indicates that the amount of immobile fraction was reduced less upon heating when more protein was present in the system. I.e. the hydration of starch seemed to be hampered by the addition of protein, which in turn could potentially influence the physicochemical properties of the starch. It is possible that, due to the relatively high solid to liquid ratio used for NMR experiments, the observed difference is simply a result of the protein absorbing water and reducing the water availability for the starch. However, further studies would be needed to clarify the mechanism behind this effect.

The assessments of water binding properties (Table 1) showed that WBC, WAI and SP of the mixtures increased as starch content increased, which may be because of increased starch content but also, as indicated

by the NMR results, because of differences in hydration efficiency between the starch and protein. Addition of gluten (Eliasson, 1983), soy (Ribotta et al., 2007) and whey (Oñate Narciso & Brennan, 2018) protein has been shown to delay diffusion of water into starch due to its presence on the surface of starch granules. The decrease in hydration efficiency with increasing content of faba bean protein may have been the result of limited water diffusion.

3.3. Hot stage microscopy

Micrographs of the different starch-protein samples at 30, 67, 73 and 90 °C are shown in Fig. 4. At 30 °C, the colour intensity, size and shape of the starch granules were similar for all samples. As the temperature

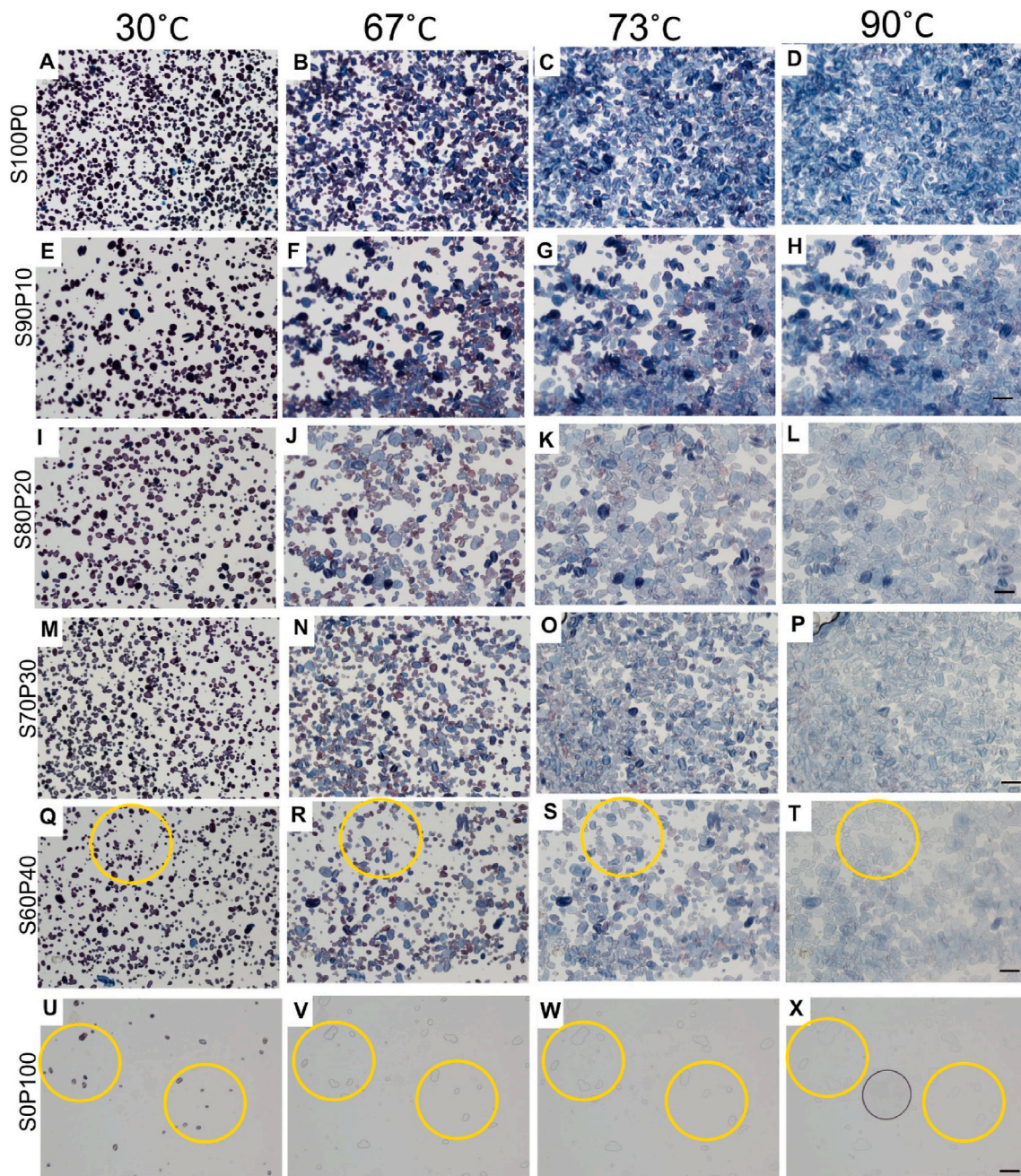


Fig. 4. Micrographs of samples S100P0 (A–D), S90P10 (E–H), S80P20 (I–L), S70P30 (M–P), S60P40 (Q–T) and S0P100 (U–X) under hot-stage microscopy at a temperature of 30 °C (first column A–U), 67 °C (second column B–V), 73 °C (third column C–W) and 90 °C (fourth column D–X). Scale bar = 100 μ m. The starch granules were stained purple/blue by iodine, with the colour intensity decreasing for each sample as the temperature increased. The yellow circles for samples S60P40 and S0P100 indicate areas where starch granules had completely lost their colour. The grey circle, as seen in figure X, indicate air bubbles.

increased the starch granules began to swell, with swelling initiating at around 63 °C and the most pronounced swelling at 70 °C. There was a gradual increase in granule size as the temperature increased to 67 °C, 73 °C and 90 °C (Fig. 4). The gradual increase in the size of the starch granules during heating is also evident in Fig. S2 in SI. From the granule size distribution, the protein-rich sample S60P40 appeared to have the smallest granules at both 30 and 67 °C, which may tie in with the NMR observation that mixture S60P40 showed slightly less efficient starch hydration. There was a tendency for the largest starch granules to be found in samples S90P10 and S80P20, indicating that addition of protein may have had a small effect in delaying granule swelling. However, this tendency was very weak overall, with no distinct difference between the populations, making it challenging to draw any direct conclusions on

whether starch swelling was delayed by the presence of protein. Furthermore, faba bean starch has a relatively high amylose content compared to many other starches (Nilsson et al., 2022). High amylose content has previously been related to retarded swelling of starch granules (Nilsson et al., 2022; Sasaki & Matsuki, 1998; Vamadevan & Bertoft, 2020). It is possible that the effect of amylose on granule swelling was affected by the presence of protein and difference in starch content between samples.

Examination under polarised light revealed that samples with starch content $\geq 60\%$ completely lost their birefringence at temperatures similar to that at which swelling occurred (around 70 °C). In the sample with no added protein (S0P100), birefringence was completely lost already at around 63 °C. Starch birefringence under polarised light is

caused by radial alignment of the crystalline amylopectin and is lost as the granules swell and lose their crystalline structure (Ambigaipalan et al., 2011; Li et al., 2019).

As the granules swelled, they became lighter and less intensely coloured. The loss of colour under progressive heating was more noticeable for the samples with higher protein content, indicating that the protein somehow interfered with or altered iodine dyeing of the starch, or that it interacted with the starch, inhibiting the formation of starch-iodine complexes. A possible explanation is that iodine formerly bound to and staining the starch granules bound to the protein instead at higher temperatures. At 95 °C, the S60P40 sample had completely lost its colour, with some of the starch granules in this sample losing their colour already at 90 °C (Fig. 4T). Areas where the starch granules in samples S0P100 and S60P40 lost their colour completely are indicated with yellow circles in the micrographs in Fig. 4. For the samples with starch content $\geq 70\%$, complete loss of colour of all granules was not observed. Samples S100P0 and S90P10 retained their colour relatively well throughout the heating (Fig. 4D and H). For sample S0P100 (Fig. 4U–X), where no starch was added to the mixture, any starch present was residual starch from protein isolation, which started to lose colour at 57 °C and lost its colour completely at around 60 °C in all micrographs.

3.4. Iodine binding capacity during heating

Fig. 5A shows the colouration of iodine staining in the different samples at different temperature intervals from 20 to 95 °C, while Fig. 5B shows the corresponding absorbance measured at 510 nm. For samples S90P10, S80P20, S70P30 and S60P40, the absorbance and observed colour intensity of the iodine staining decreased as the temperature of the mixture increased. As already observed in the hot-stage micrographs, the loss of colour was more prominent in the samples with higher protein content, with complete loss of colouration occurring at lower temperatures (50 °C for S60P40, 60 °C for S70P30, 70 °C for S80P20 and 80 °C for S90P10). For the pure starch sample S100P0, the measured absorbance remained constant up to and including 60 °C, while at 70 °C the absorbance peaked before decreasing. In a previous study, we found that gelatinisation of faba bean starch extracted from the same batch of raw beans occurred between 67 and 73 °C (Nilsson et al., 2022), so increased granule size might explain the observed peak in absorbance. As the temperature continued to increase measured absorbance decreased but, unlike in the other samples, there was no complete loss of colour for sample S100P0.

To verify that the loss in colour in the protein-rich samples was not due solely to the lower concentration of starch, a new sample S60P0 was prepared containing the same quantity of starch as the S60P40 sample but without any added protein (i.e. the overall solids content was lower). Sample S60P0 showed similar behaviour to the pure starch sample

S100P0, with iodine colouration better maintained and not completely lost at higher temperatures. Hence, the loss in colour was not simply a consequence of the reduced starch content in the mixed samples.

Unheated starch in contact with iodine turns into a characteristic blue-black colour, as the iodine forms complexes inside the long helical chains of linear amylose. The highly branched amylopectin, with much shorter but more numerous chains, turns into a reddish-brown colour upon contact with iodine (Holló & Szejtli, 1958; Huber & Bemiller, 2017). Loss of colour of starch-iodine mixtures upon heating is a well-known phenomenon believed to be caused by the complex decomposing at elevated temperatures (Fonslick & Khan, 1989). The starch-iodine reaction has an exothermic equilibrium, with the iodine colouration recovering upon cooling. However, for the starch-protein mixtures in this study, the discolouration caused by heating did not recover after the samples were cooled, indicating that some interaction between protein-iodine and/or protein-starch prevented the reaction from returning to its original equilibrium. There was also no recovery of colour for the pure starch sample when tested at a lower iodine concentration (200 μ L Lugol's solution instead of 2 mL) (Fig. S3 in SI). On adding iodine to the cooled samples, the mixtures turned blue-black again.

One possible explanation for the observed loss of colour is that the protein in the samples had a higher affinity for iodine than the starch, resulting in less iodine binding to starch in the presence of protein. The lower iodine concentration tested here resulted in loss of colour upon heating that was relatively similar to that seen for S60P40 (Fig. S3). Other possible explanations are complex formation between the starch and protein or protein adsorption on the surface of starch granules, preventing the iodine from binding to amylose. Encapsulation of corn starch granules by whey protein has been reported (Yang, Zhong, Goff, & Li, 2019). The iodine dyeing intensity may also be reduced if the amylose spiral cavity is occupied by guest molecules, thus hindering amylose-iodine complex formation. Further tests involving mixing the starch and Lugol's solution before addition of protein, compared with mixing the starch and protein before addition of Lugol's solution, resulted in a delay in observed colour loss as the temperature increased (Fig. S3). This indicates that competition for iodine is the more likely explanation for the observed loss of colour, with iodine previously complexed with starch instead bonding with the protein as the complex decomposed because of heating, and remaining bound to protein and no longer available to form a complex with starch again after cooling, resulting in the cooled mixture remaining discoloured. However, further studies are needed to fully identify the mechanism behind the observed loss in colour.

3.5. Pasting

Fig. 6 shows the pasting curves of the starch-protein mixtures during

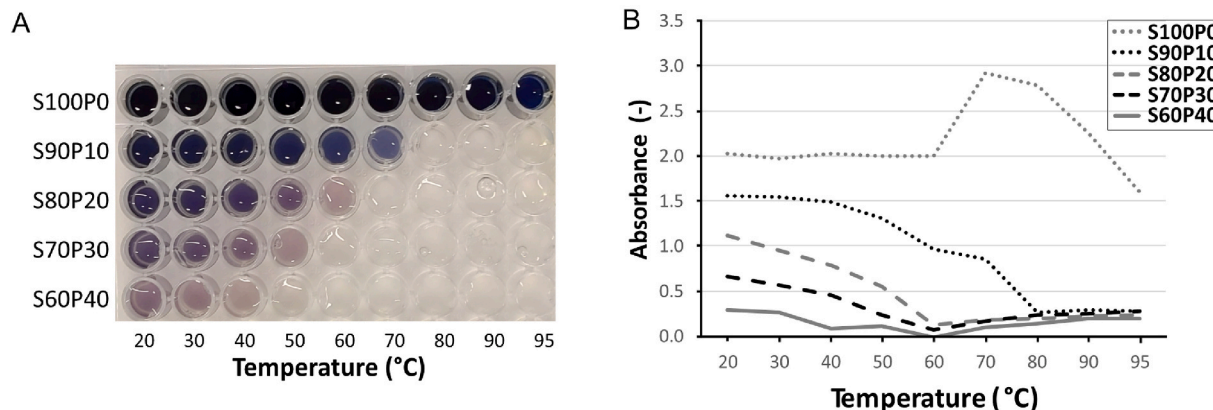


Fig. 5. (A) Image of iodine-stained starch-protein (S%:P%) mixtures at different temperatures and (B) corresponding absorbance measured at 510 nm.

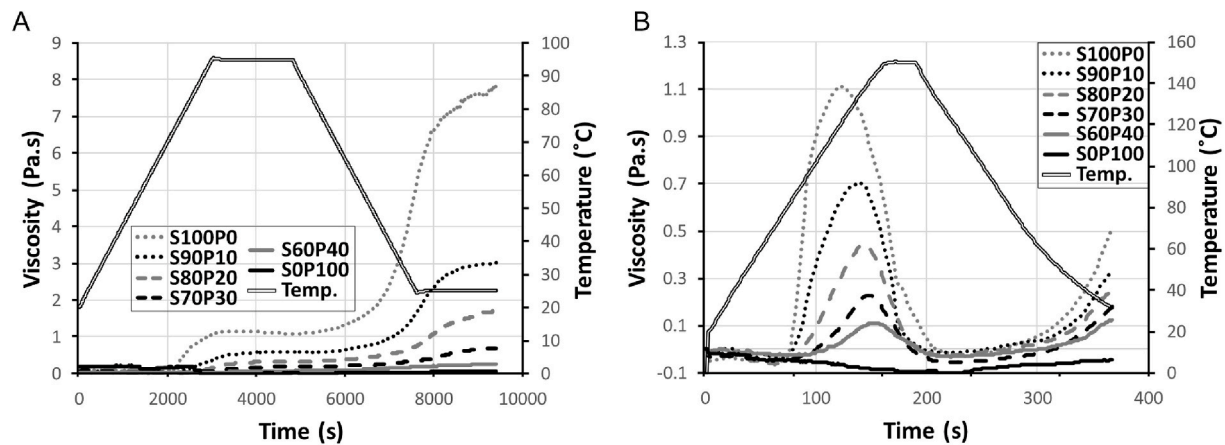


Fig. 6. Pasting curves of the starch-protein (S%P%) mixtures on heating to (A) maximum temperature 95 °C and (B) maximum temperature 150 °C.

heating to 95 °C and 150 °C. Although the shape of the curves differed, both graphs show that apparent pasting viscosities increased with higher starch content. This was observed from the thickness of the pastes already during analysis in the laboratory. At both temperatures, the SOP100 sample had the lowest final viscosity and did not form a gel in the pressure cell. Samples S60P40 and S70P30 formed viscous soft gels, while samples with starch content $\geq 80\%$ formed cohesive gels. Another observation from the pasting analyses was that pasting was initiated at lower temperatures when the sample contained more starch.

In the pasting curves for heating to 95 °C (Fig. 6A), pasting commenced at around 73.2 °C for sample S100P0. For sample S90P10, the pasting temperature increased to 78.3 °C and for sample S60P40 it was 89.9 °C. For the pure protein sample SOP100, the pasting temperature could not be determined, as no pasting occurred. An absence of peak viscosity was observed during pasting experiments with heating to 95 °C. This is in line with previous results on faba bean starch and could possibly be related to the high amylose content which could help maintain the granular integrity (Hoover, Hughes, Chung, & Liu, 2010; Nilsson et al., 2022). Samples with a starch content of $\geq 70\%$ showed a plateau during the holding time after the initial viscosity increase in the cooling phase (Fig. 6, Fig. S4 in SI). For sample S60P40, the viscosity increased steadily throughout the experiment. Increased protein content in the samples delayed the onset time for the second increase in viscosity in the samples. The second onset temperature, when the viscosity increased again during the cooling phase in the pasting analysis, was 31.6 °C for sample S70P30 and 42.1 °C for sample S100P0. From these results, it is not possible to conclude whether the difference in pasting temperature between the starch-rich and protein-rich samples was a result of the two components interacting or an effect of the starch-rich gels having overall higher viscosity.

Heating the samples to 150 °C was sufficient to achieve peak viscosity, followed by breakdown of the paste (Fig. 6B). The final viscosities in the 150 °C measurements were much lower than those in the 95 °C measurements (Table S1 in SI). The lower final viscosities in the high-temperature pasting analysis were presumably because of substantial granule breakdown on heating to 150 °C compared with 95 °C (Nilsson et al., 2022). However, the difference in heating/cooling rates and holding time at 25 °C limited comparison of the results of the different pasting experiments.

As the protein content increased, the temperature at which peak viscosity occurred also increased and the peak viscosity decreased (Fig. 6B, Table S1). The peak viscosity was highest (1.11 Pa s) for the pure starch sample S100P0 and was reached at 121 °C, while for sample S60P40 peak viscosity was 0.11 Pa s and was reached at 145 °C. Moreover, the breakdown viscosity of the samples increased with increasing starch content, most likely due to the higher peak viscosities of the more starch-rich samples. However, well-maintained viscosity

during the heating and cooling may also suggest molecular entanglement between starch and/or protein molecules in the paste (Onwulata et al., 2014).

3.6. Oscillatory rheology

Storage modulus (G') was monitored during gel formation (Fig. 7). The increase in G' seen during initial heating seemed to occur earlier as the starch content increased. At a starch content of 80% (of total flour added) or higher, the gels showed a peak in G' during heating and changes during cooling more similar to those in the pure starch gels. At lower starch contents, the peak observed during heating was not visible, and the changes in G' were more similar to those in the pure protein gels.

The loss modulus (G'') showed a similar pattern to G' (Fig. S5 in SI). Except in the pure protein gels, G'' was lower than G' throughout the whole gelation process. In the pure protein gels, G'' exceeded G' during the initial part of the measurement, before gelation of the sample occurred. G' , G'' , $\tan \delta$ and end of LVR of the final gels are summarised in Fig. 7B–E and Table S2 in SI.

Both G' and G'' decreased with increasing protein content. $\tan \delta$ of the final gels increased with increasing protein content, indicating less solid-like behaviour of the gels. Except for the pure protein gels, the amplitude sweep showed a decrease in LVR with increasing protein content. Large deformation properties, such as the structural breakdown occurring at high amplitudes during an amplitude sweep, may be affected by inhomogeneities and structural defects (Dille, Draget, & Hattrem, 2015; Munialo et al., 2014). Hence, the reduced LVR for the mixed systems could be related to inhomogeneities in the gel network created by either the starch, the protein or both. The amplitude sweep also showed a more distinct breaking point at the end of LVR with increasing starch content (Fig. S6 in SI), indicating more clear and brittle fracturing of the starch-rich gels. In contrast, the samples with higher protein content showed a more gradual decay in G' as the strain increased, indicating more creamy behaviour.

The changes in G' during gelation showed a relatively similar pattern to those of the pasting curves at 95 °C. However, the peak observed during heating of the starch-rich samples in the oscillatory measurements (highlighted with arrows in Fig. 7A) was not observed during pasting at 95 °C, which may be attributable to the continuous shearing occurring for the pasting measurements potentially being more disruptive for gel formation. The differences between pasting and oscillatory rheology data observed in the initial part of the measurements, as well as any potential differences between the pure protein gels, should be interpreted with caution, due to the erratic data obtained at low torques.

The changes in G' observed for the pure protein gel were similar, but lower in absolute terms, to those previously reported for faba bean protein at higher protein concentrations (Johansson, Johansson, et al.,

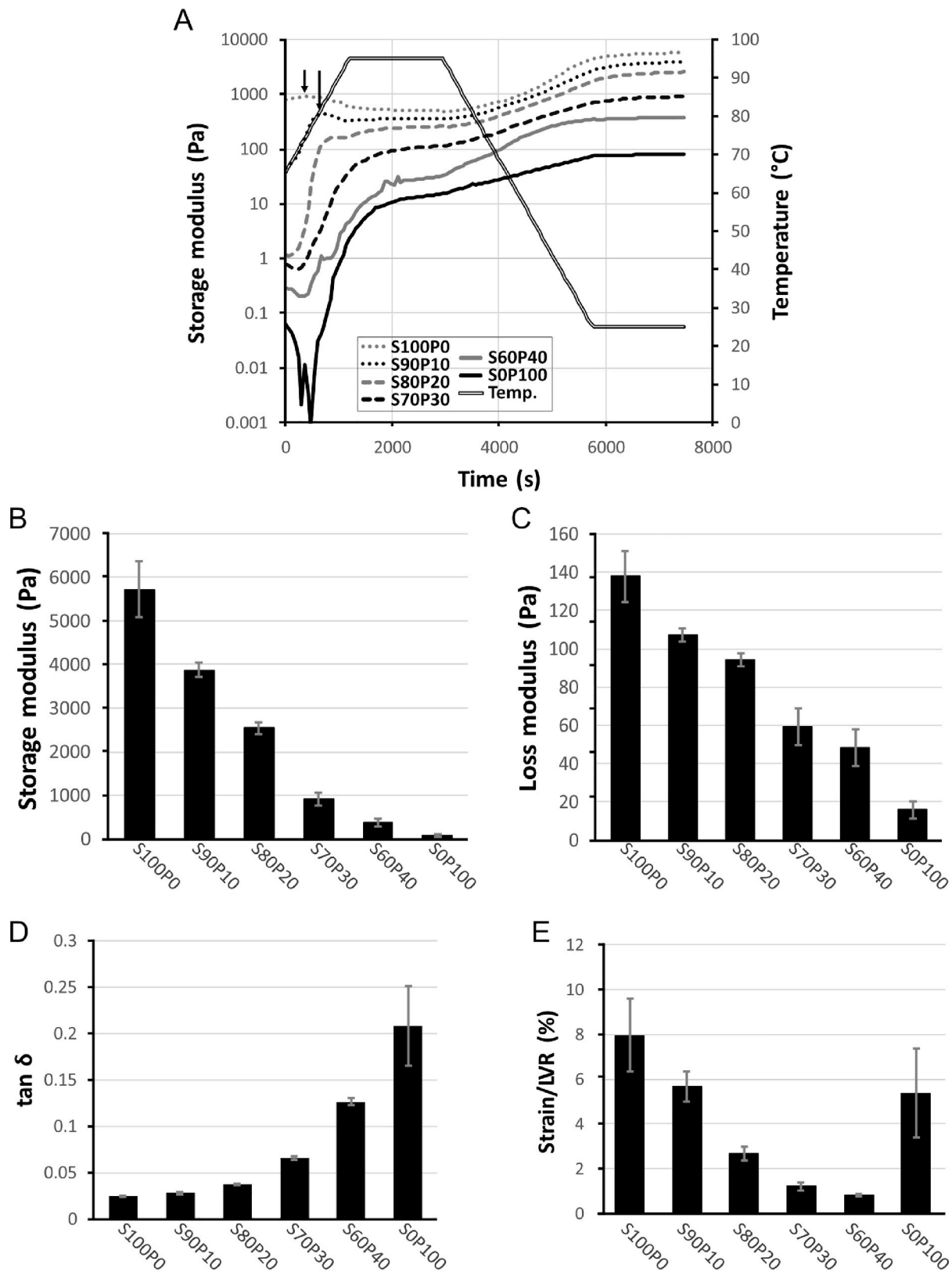


Fig. 7. (A) Storage modulus during temperature ramp for the different starch-protein (S%P%) composites. (B–D) Storage modulus, loss modulus and tan δ obtained from the final time point of the temperature ramp in A. (E) End of the linear viscoelastic region (LVR) measured on the final gels after the temperature ramp. Error bars represent ±1 st.dev.

2022; Langton et al., 2020). As the starch content in the mixtures here increased, G' also increased and a gradual shift towards the behaviour of the pure starch sample was observed (Fig. 7A). A similar increase in G' throughout the gelation process has been observed previously for faba bean starch-protein systems, although at higher total solids content and lower proportions of starch (Johansson et al., 2022a).

An increase in G' with increasing starch:protein ratio has previously been reported for lentil starch:protein gels (Joshi et al., 2014). However, the opposite has been observed for potato protein:potato starch gels, with an increase in the proportion of starch reducing the G' value of the gels (Zhang, Mu, & Sun, 2017). These results indicate that the properties and behaviour of starch-protein gel systems depend on the source and properties of the starch and protein used.

A study by Muhrbeck and Eliasson (1991) on the rheological properties of starch-protein mixtures from different sources revealed that the transition temperature and gelation rate of the two components were critical for the behaviour of the mixed system. In brief, it was shown here, that if the starch gelled before the protein, the rheological properties of the mixed gel system could be predicted by simple addition of the modulus values of its individual components. If the protein gelled before the starch, the system showed higher modulus values than predicted by simple addition of its components. The faba bean starch used in the present study has a gelatinisation temperature below the denaturation temperature of the protein (75–95 °C) (Kimura et al., 2008), and can be assumed to gel first. This assumption was supported by laboratory observations that gels with a higher fraction of starch were noticeably more viscous after the pre-heating step at 65 °C. Hence, the decrease in G' in the gels as the starch content decreased seems to be in line with observations by Muhrbeck and Eliasson (1991), i.e. that increased protein concentration leads to lower G' of the mixed system, since protein forms weaker gels than starch, and that G' of the mixed system can be predicted by adding together the modulus values for its individual components.

The gels were further characterised by a frequency sweep (Fig. 8). The dependence of G' on frequency was evaluated by calculating the relaxation exponent (n) after fitting the data to a power law equation, $G' = S\omega^n$, where S and n are constants and ω is the angular frequency (Chambon & Winter 1987; Tanger, Müller, Andlinger, & Kulozik, 2022; Winter & Chambon, 1986). A purely elastic material is frequency-independent, with $n = 0$ (Alting, Hamer, De Kruif, & Visschers, 2003), and gel networks formed by mainly chemical cross-links will have a relaxation exponent close to zero (Tanger et al., 2022). A gel network formed by mainly secondary bonds (e.g. hydrogen bonding and hydrophobic interactions) will have a slightly higher frequency dependence (Tanger et al., 2022). A small contribution from the viscous component (G'') is typical for food gels. This contribution results in a frequency dependence of G' reflecting relaxation of the viscous components (Alting et al., 2003).

In this study, G' was higher than G'' for all samples over the full frequency range analysed (Fig. 8A and B), indicating mainly elastic deformations (Zhang et al., 2017). The n -values of the gels indicated that interactions within the gel network were mainly of a physical nature. The n -values increased with increasing protein content. This increased frequency dependence is in agreement with the increase in $\tan \delta$, reflecting the more viscous behaviour of the protein-rich gels, indicating weaker gel structure (Vogelsang-O'Dwyer et al., 2020).

The G'' values indicated stronger frequency dependence compared with G' , as evidenced by the higher n -values (Table 2). Overall, similar trends were observed for n -values calculated for both G' and G'' . As found for G' , both similar and opposing trends in n -values with increasing starch:protein ratio have been observed for other starch-protein sources (Gui et al., 2022; Joshi et al., 2014; Zhang et al., 2017). However, it could be noted that for all these cases, the gels with the highest G' gave the lowest n -values. This is in line with the lower frequency dependence typically observed for stronger and less fluid like gels (Vogelsang-O'Dwyer et al., 2020).

3.7. Compression tests

Compression tests were used to investigate the textural properties of the gels. All characteristics evaluated (fracture stress, fracture strain, Young's modulus) showed a decrease with increasing protein content (Fig. 9, Table S3). The gels with 60% starch and 40% protein (S60P40) were not completely homogenous, with more solid-like behaviour towards the lower part of the gel due to partial sedimentation of the starch, so the middle part of these gels was used for compression tests. The gels containing only protein were not self-standing and could therefore not be analysed by compression tests.

Fracture stress, fracture strain and Young's modulus decreased with increasing protein content. The fracture and fracture point were more distinct for the gels with higher starch content, showing a clear drop in force as the gels fractured (Fig. S7 in SI). The gels with higher protein

Table 2

n -values (mean \pm 1 st.dev.) for the different starch-protein (S%P%) gels. Values obtained after fitting frequency sweep data (storage (G') and loss modulus (G'')) to the equation: Storage/loss modulus = $S\omega^n$, where S and n are constants and ω is the angular frequency. Different superscript letters indicate significant differences within columns ($p < 0.05$).

Sample	n (G')	n (G'')
S100P0	0.016 \pm 0.000 ^a	0.197 \pm 0.004 ^a
S90P10	0.019 \pm 0.001 ^a	0.198 \pm 0.003 ^a
S80P20	0.024 \pm 0.001 ^b	0.200 \pm 0.005 ^a
S70P30	0.038 \pm 0.001 ^c	0.234 \pm 0.023 ^a
S60P40	0.069 \pm 0.002 ^d	0.249 \pm 0.032 ^a
S0P100	0.134 \pm 0.022 ^e	0.291 \pm 0.054 ^a

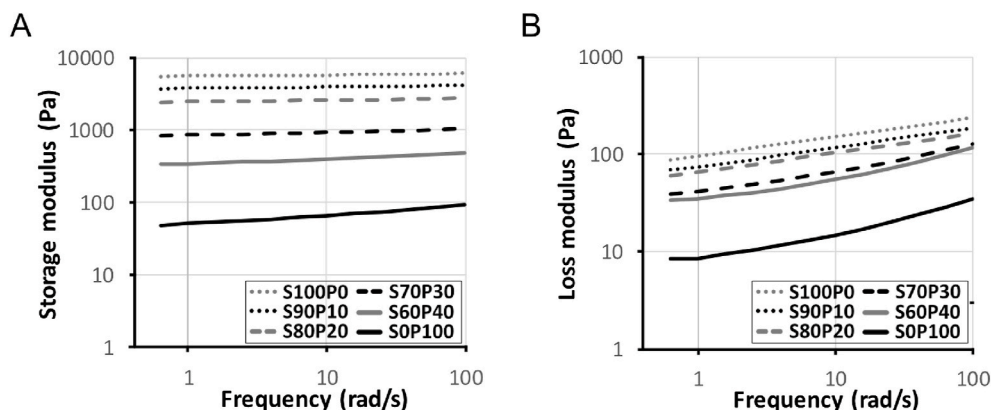


Fig. 8. (A) Storage modulus and (B) loss modulus as a function of frequency for the different starch-protein (S%P%) gels.

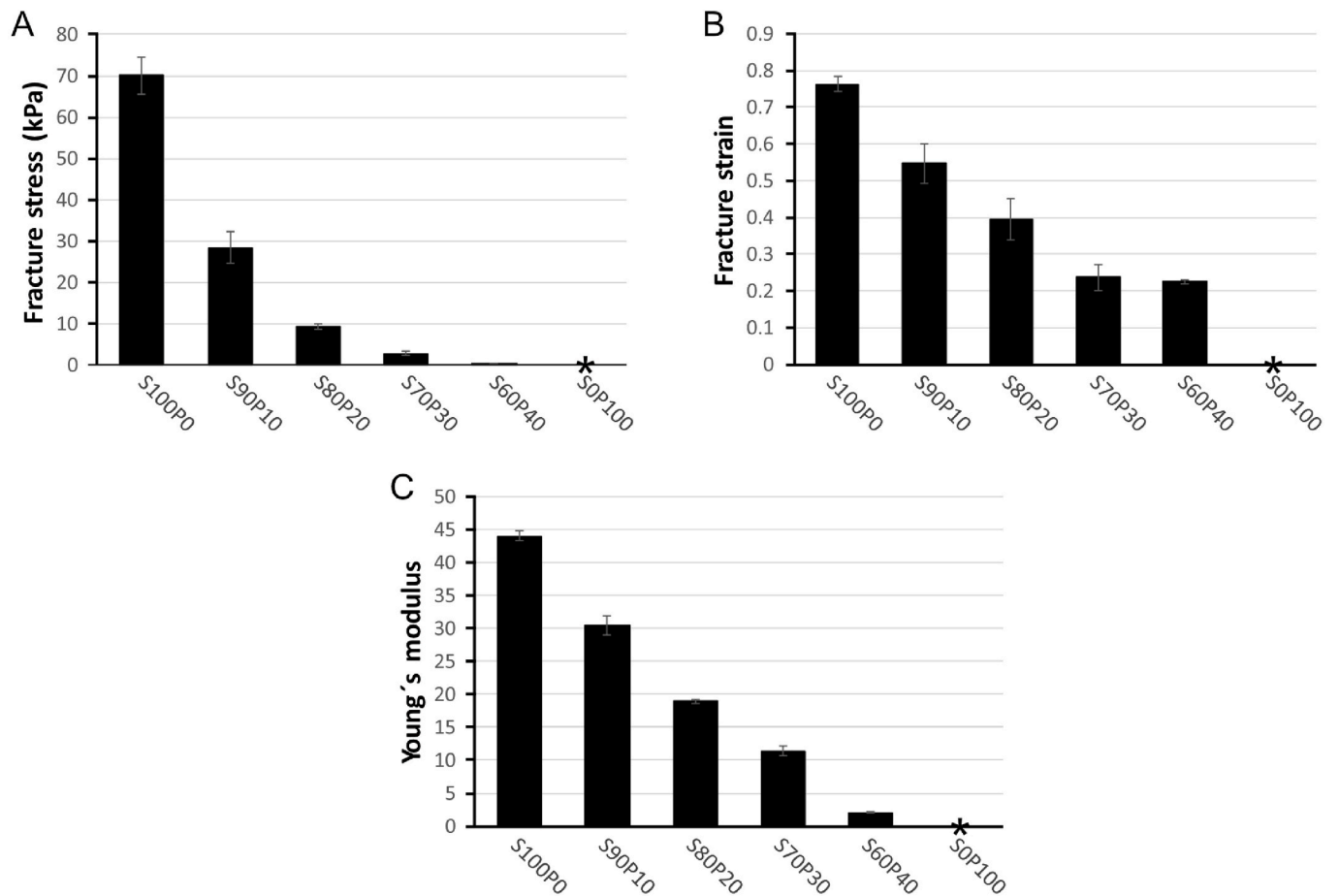


Fig. 9. (A) Fracture stress, (B) fracture strain and (C) Young's modulus of the different starch-protein (S%P%) gels analysed by compression tests. Error bars represent ± 1 st.dev. *Sample did not form self-standing gels and could not be measured.

content showed more ductile behaviour and less clear fracture. The more distinct fracture of the starch-rich gels was also observed visually during compression tests, where starch-rich samples ($\geq 80\%$ starch) fractured into well-defined/separate pieces, whereas gels with $\leq 70\%$

starch did not break into separate pieces and showed more paste-like behaviour upon fracture.

As expected, the Young's modulus and fracture strain values from compression tests showed similar trends to those observed for G' and

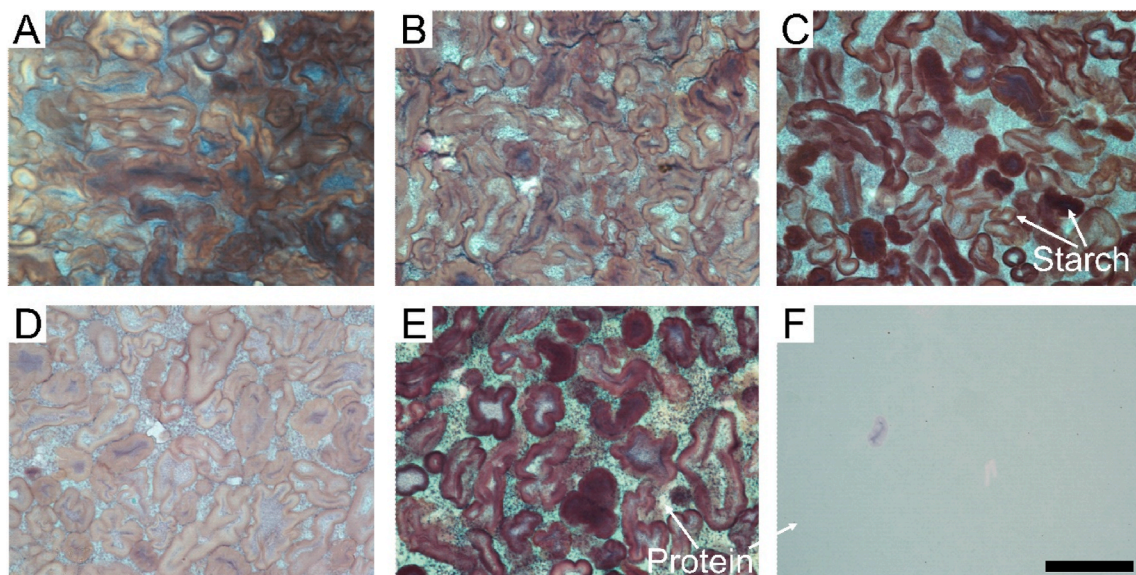


Fig. 10. Light microscopy micrographs of the starch-protein (S%P%) gels. (A) S100P0, (B) S90P10, (C) S80P20, (D) S70P30, (E) S60P40 and (F) S0P100. Scale bar = 50 μm .

LVR during oscillatory rheology measurements. The more clear and distinct fracture observed during compression of starch-rich gels (Fig. S7) was in agreement with the clearer drop in G' at higher strains observed in the strain sweep (Fig. S6).

Previous studies on faba bean starch-protein gels have reported lower fracture stress and fracture strain with increasing starch content (Johansson, Johansson, et al., 2022). However, those gels contained mainly protein, with a maximum starch:protein ratio of 35:65, and had a higher solids content (20%) than in this study (12%). Firmer gel consistency with increasing starch:protein ratio has previously been reported for lentil starch:protein gels (Joshi et al., 2014).

3.8. Microstructural characterisation of gels

3.8.1. Light microscopy

Gel microstructure was characterised by light microscopy with protein stained in blue/green and starch in brown/purple (Fig. 10). The micrographs indicated that starch-rich gels were more densely packed with starch, which could explain the observed firmness of starch-rich gels during compression tests, higher elastic modulus in oscillatory rheology and higher viscosity development in pasting analysis. The protein fraction was more evident in gels with higher protein content. The starch granules appeared to be the continuous phase for all gels with starch content $\geq 70\%$. For the S60P40 gel samples, the continuous phase was more difficult to define (Fig. 10E), with the starch and protein potentially forming two separate bicontinuous networks.

For the gels with higher protein content, the leaked amylose seemed to aggregate into more amylose-dense regions (darker blue spots) within the protein network (Fig. 11). Amylose aggregates within a continuous protein network have been observed previously in mixed faba bean protein:starch gels with higher protein content (protein $\geq 65\%$) and solids content (20%) (Johansson, Johansson, et al., 2022). For the gels with starch content $\geq 90\%$, the amylose seemed to form a gradually finer network, rather than the larger aggregates observed in the gels with higher protein content (Fig. 11). This amylose aggregation into clusters rather than a network could relate to the observed reduction in storage modulus, fracture stress and fracture strain with increasing protein content. Aggregation of amylose has been shown to occur in other mixed systems (starch-emulsifier), indicating that it is due to phase separation rather than amylose-protein complex formation (Richardson, Kidman, Langton, & Hermansson, 2004). The phase separation occurring

between the amylose and protein might be related to differences in their hydrophobicity. Most plant proteins, including the majority of faba bean proteins, are globular proteins and tend to become more hydrophobic upon denaturation (Kim, Wang, & Selomulya, 2020). However, upon denaturation, the protein gel network will also start to form and mobility within the system will be reduced. Hence, any phase separation occurring before gelation might be permanently captured within the gelled structure (Yang, Liu, Ashton, Gorczyca, & Kasapis, 2013).

Previous studies have suggested that protein in mixture gels may perturb starch network formation, thereby weakening the gel (Bravo-Núñez et al., 2019; Bravo-Núñez & Gómez, 2019; Joshi et al., 2014; Oñate Narciso & Brennan, 2018; Onwulata et al., 2014). The compression test results here showed a strong correlation between high starch content and increased firmness, which could be explained by higher protein content disrupting the starch gel network and producing a heterogeneous and weaker gel. The sequence of gel formation has been found to influence the microstructure of lentil starch-protein mixed gels, with the starch becoming more viscous than the protein at lower temperatures (Joshi et al., 2014). Similar behaviour could be expected for faba bean gels, as faba bean starch has a lower gelatinisation temperature than the denaturation temperature of faba bean protein.

3.8.2. SEM

Gel microstructure characterisation by SEM revealed that gels with $\geq 80\%$ starch had regions with a more porous network structure than gels with less starch (Fig. 12, Fig. S8 in SI). In general, the continuous network of these gels showed a structure more similar to the pure starch gels, while the network of gels with $\leq 70\%$ starch showed a denser structure more similar to that of the pure protein gels. Examples of regions with porous and dense network structures are highlighted with arrows in Fig. 12. For gels containing starch, starch granules and cavities where starch granules had been present were evident throughout the structure. In general, a denser and finer network structure was observed around these cavities.

In the LM micrographs, starch was the most visible and dominant component of all samples except the pure protein gels. Despite this, the microstructure of S70P30 and S60P40 gels showed a greater resemblance to the pure protein gels when observed by SEM. The gels with $\geq 30\%$ protein largely lacked the less dense and more fibrous and stranded structure observed in the starch-rich gels. This was possibly due to the fracturing of samples performed before analysis to expose the

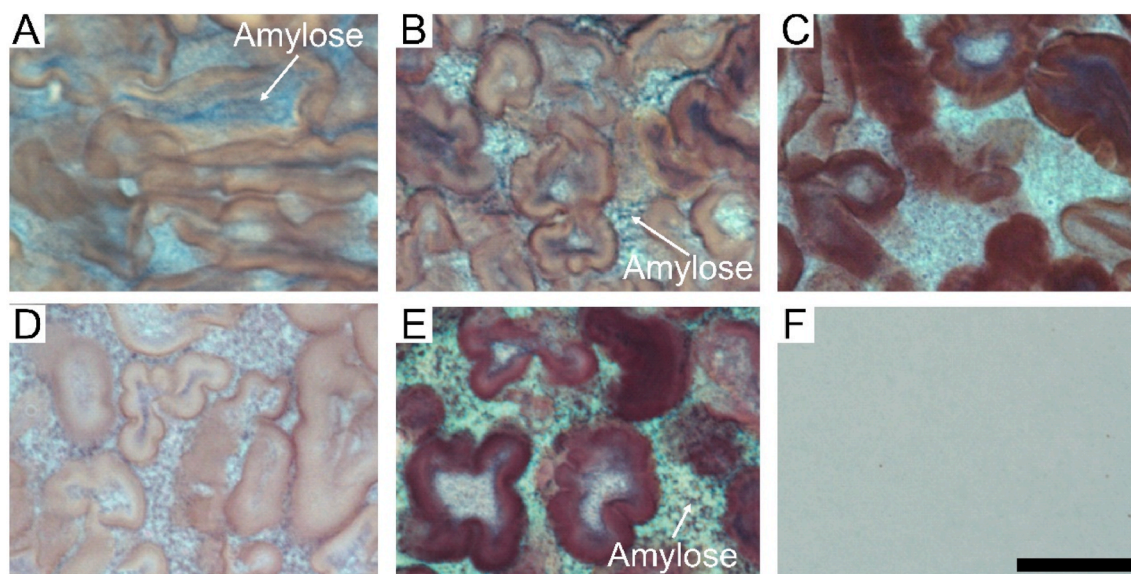


Fig. 11. Magnified views of the micrographs in Fig. 10. (A) S100P0, (B) S90P10, (C) S80P20, (D) S70P30, (E) S60P40 and (F) S0P100. Scale bar = 25 μm . Data size: 975 \times 731 pixels.

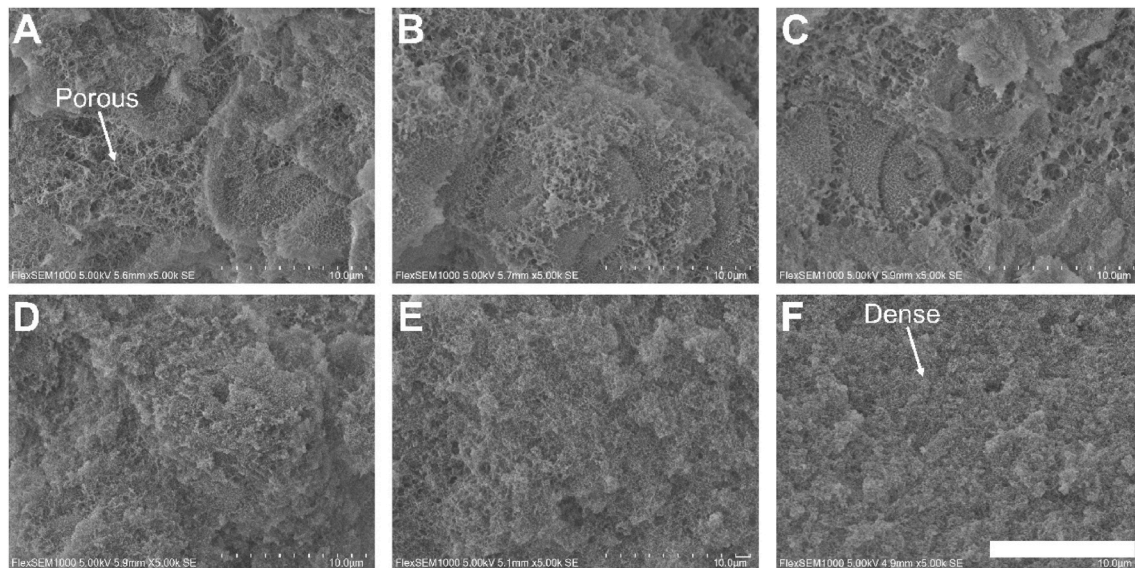


Fig. 12. Scanning electron microscopy (SEM) micrographs of the starch-protein (S%P%) gels. Examples of regions with porous or dense network structures are highlighted with arrows. (A) S100P0, (B) S90P10, (C) S80P20, (D) S70P30, (E) S60P40 and (F) S0P100. Scale bar: 10 μm .

inner part of the fixed gel, with fractures propagating mainly through the weakest regions of the structure. Since the protein-rich regions were likely to be weaker than the network formed by the starch, fracturing was more likely to occur through these regions. This could explain why the samples with $\geq 30\%$ protein showed such high similarity to the pure protein gels despite their high starch content and why the starch was clearly evident in the LM micrographs of corresponding gel samples.

3.9. Overall trends and correlations

Overall, the results showed that gel morphology/structure and properties were highly dependent on the starch:protein ratio in the mixture. A comprehensive overview of the relationships between morphology/structure and properties of starch-protein mixtures is provided by Zhang et al. (2021). To summarise, higher protein content in the faba bean starch-protein samples resulted in lower pasting viscosities, less firm gels and a more compact and less fibrous gel structure, with the starch appearing to aggregate into clusters. Hydration was also less efficient for the high-protein mixtures. These effects became more pronounced as the protein content of the samples increased.

Apparent viscosity and firmness were strongly positively correlated for high-starch samples, e.g. there was a strong correlation ($r = 0.98$, $p < 0.001$) between peak pasting viscosity and elastic modulus in the rheological temperature ramp. Gels with a higher proportion of protein were also more frequency-dependent, which indicates a weakened gel structure (Joshi et al., 2014).

More efficient hydration and higher iodine absorbance were also positively correlated with higher paste viscosity and firmer gel ($r = 0.97$; $p < 0.001$ for the correlation between WAI and peak viscosity, $r = 0.85$; $p = 0.003$ for that between WAI and elastic modulus). The less efficient hydration properties of the gels containing protein could have affected the distribution of water within the starch-protein matrix and affected molecular interactions. A lower water holding capacity, as observed for the gels containing protein, can lead to lower textural stability (Boye, Zare, & Pletch, 2010). Proteins competing with starch for water may limit granule swelling by restricting water absorption, thereby reducing apparent viscosity (Eliasson, 1983; Oñate Narciso & Brennan, 2018; Ribotta et al., 2007). As indicated by the hot-stage microscopy micrographs (see Fig. 4 and Fig. S2), there was a tendency for slightly less intense swelling in the high-protein samples. The NMR results (Fig. 3) confirmed that hydration was slightly less efficient for sample S60P40

compared with S90P10. Slower absorption of water may also lead to delayed pasting because of retarded swelling of the starch granules causing less granule contact.

The more prevalent iodine colour loss associated with higher protein content (see Figs. 4 and 5) indicates that the protein formed a complex with the starch or bound the iodine, rendering it unavailable to form complexes with the starch. If protein-starch complexes are formed, consequences could be delayed granule hydration and swelling and a reduction or perturbation in starch-starch network development.

Another plausible explanation for higher protein content resulting in reduced paste viscosity (Fig. 6) and less firm gels (Fig. 9) is dilution of the starch by the protein, as starch often has better gelling properties, forming stronger gels, than protein (Bravo-Núñez et al., 2019; Bravo-Núñez & Gómez, 2019). The LM micrographs (Figs. 10 and 11) showed that starch granules were more tightly packed in the high-starch gels. However, viscosity differences exceeded actual starch dilution, suggesting that the protein somehow interfered with viscosity development of the starch.

In the SEM micrographs (Fig. 12), the starch-rich gels displayed regions with a more porous and fibrous network. The oscillating frequency results, with higher calculated n -value for samples with higher protein content, indicated greater presence of secondary bonds (Tanger et al., 2022), which in turn could lead to denser network structure because of less bonding between the starch chains. Starch gel matrices consist of swollen granules, entangled polymer chains and non-covalent interactions (Larrea-Wachtendorff, Del Grosso, & Ferrari, 2022; Walstra, 2002). Ribotta et al. (2007) concluded that soy protein can interact readily with amylose and exposed branches of amylopectin through non-covalent bonding, especially hydrogen bonds, causing further gel matrix weakening.

Proteins may act as an inert filler, hindering realignment of the starch chains during gelation. An effect of protein addition in altering microstructure and reducing viscosity and/or gel strength has been reported for numerous starch-protein mixtures, such as wheat starch-soy protein (Ribotta et al., 2007), starch-dairy (Yang et al., 2004) and various starch-plant/animal-based proteins (Bravo-Núñez et al., 2019; Bravo-Núñez & Gómez, 2019). A previous study analysing the same starch as used in this study revealed that the amylose content was 32.2% (Nilsson et al., 2022). The effect of protein in decreasing viscosity and gel strength has been shown to be greater for amylose-rich starches, as the proteins are more likely to interfere with re-ordering of the amylose

(Bravo-Núñez et al., 2019; Joshi et al., 2014; Oñate Narciso & Brennan, 2018). Amylose re-ordering into clusters, rather than developing into a network, in the presence of emulsifiers has also been found to have a weakening effect (Richardson, Kidman, et al., 2004; Richardson, Sun, Langton, & Hermansson, 2004). As observed from the LM micrographs (Figs. 10 and 11), similar re-ordering into clusters rather than a network seemed to occur for the gels in this study as the protein content increased.

The overall effect on pasting and gel structure matrix is also dependent on the type of protein incorporated (Zhang et al., 2021). The pure protein mixtures (SOP100) in this study formed very weak gels, as indicated by the rheological results (Figs. 6 and 7), compression results (Fig. 9) and LM micrographs (Figs. 10 and 11), so the protein in the mixed systems likely did not create any strong network contributing to the overall strength of the mixed systems. The lowest gelling concentration of faba bean protein is reported to be around 13–14% (Fernández-Quintela, Macarulla, del Barrio, & Martínez, 1997; Langton et al., 2020), which is higher than in the mixtures here (12% solids).

4. Conclusions

A decrease in the proportion of starch in faba bean starch-gel mixtures, while keeping the solids content (starch + protein) constant, resulted in lower measured viscosities during pasting. Gels with decreased starch content (and increasing protein content) also showed a decrease in storage modulus, fracture stress, fracture strain and Young's modulus. The water binding and hydration properties of the starch-protein mixtures improved with higher starch content, suggesting that water binding and gel rheological values may be related. Changes in textural and rheological properties appeared to occur gradually over the starch:protein ratios tested. Light microscopy indicated that starch was the continuous phase, consisting of swollen granules, for gels with starch content $\geq 70\%$ of total solids and that starch and protein potentially formed two bicontinuous networks at a starch content of 60%. Scanning electron microscopy revealed a more porous starch network, with thicker strands than in the protein network. In general terms, it can be stated that the textural properties, and in turn also the mouthfeel and perception, of starch-protein gels depend largely on the starch to protein ratio in the system. To produce a stable and brittle gel a higher starch content may be desirable, while to produce a softer and perhaps pourable gel a higher proportion of protein may be preferred. However, if the solids content in the gels (12%) had exceeded the lowest gelling concentration of faba bean protein (14%), their properties may have been different.

CRedit authorship contribution statement

Klara Nilsson: Conceptualization, Formal analysis, Investigation, Methodology, Validation, Visualization, Writing – original draft, Writing – review & editing. **Mathias Johansson:** Conceptualization, Formal analysis, Investigation, Methodology, Validation, Visualization, Writing – original draft, Writing – review & editing. **Corine Sandström:** Investigation, Methodology, Writing – review & editing. **Hanna Eriksson Röhnisch:** Investigation, Writing – review & editing. **Mikael S. Hedenqvist:** Writing – review & editing. **Maud Langton:** Conceptualization, Funding acquisition, Methodology, Supervision, Writing – review & editing.

Declaration of competing interest

None.

Data availability

Data will be made available on request.

Acknowledgements

This work was supported by the FORMAS [grant numbers 2018–01869, 2017–00426]; and Trees and Crops for the Future (TC4F), a Strategic Research Area at SLU, supported by the Swedish Government.

Appendix A. Supplementary data

Supplementary data to this article can be found online at <https://doi.org/10.1016/j.foodhyd.2023.108494>.

References

- Alting, A. C., Hamer, R. J., De Kruijff, C. G., & Visschers, R. W. (2003). Cold-set globular protein gels: Interactions, structure and rheology as a function of protein concentration. *Journal of Agricultural and Food Chemistry*, 51(10), 3150–3156. <https://doi.org/10.1021/jf0209342>
- Ambigaipalan, P., Hoover, R., Donner, E., & Liu, Q. (2013). Retrogradation characteristics of pulse starches. *Food Research International*, 54(1), 203–212. <https://doi.org/10.1016/j.foodres.2013.06.012>
- Ambigaipalan, P., Hoover, R., Donner, E., Liu, Q., Jaiswal, S., Chibbar, R., et al. (2011). Structure of faba bean, black bean and pinto bean starches at different levels of granule organization and their physicochemical properties. *Food Research International*, 44(9), 2962–2974. <https://doi.org/10.1016/j.foodres.2011.07.006>
- Aschemann-Witzel, J., Gantriis, R. F., & Fraga, P. (2021). Plant-based food and protein trend from a business perspective: Markets, consumers, and the challenges and opportunities in the future. *Critical Reviews in Food Science and Nutrition*, 61(18), 3119–3128. <https://doi.org/10.1080/10408398.2020.1793730>
- Boye, J., Zare, F., & Pletch, A. (2010). Pulse proteins: Processing, characterization, functional properties and applications in food and feed. *Food Research International*, 43(2), 414–431. <https://doi.org/10.1016/j.foodres.2009.09.003>
- Bravo-Núñez, A., Garzón, R., Rosell, C. M., & Gómez, M. (2019). Evaluation of starch-protein interactions as a function of pH. *Foods*, 8(5), 155. <https://doi.org/10.3390/foods8050155>
- Bravo-Núñez, A., & Gómez, M. (2019). Physicochemical properties of native and extruded maize flours in the presence of animal proteins. *Journal of Food Engineering*, 243(August 2018), 49–56. <https://doi.org/10.1016/j.jfoodeng.2018.09.005>
- Chambon, F., & Winter, H. H. (1987). Linear viscoelasticity at the gel point of a crosslinking PDMS with imbalanced stoichiometry. *Journal of Rheology*, 31(8), 683–697. <https://doi.org/10.1122/1.549955>
- Dille, M. J., Dragnet, K. I., & Hattrem, M. N. (2015). 9 - the effect of filler particles on the texture of food gels. In J. Chen, & A. Rosenthal (Eds.), *Modifying food texture* (pp. 183–200). Woodhead Publishing. <https://doi.org/10.1016/B978-1-78242-333-1.00009-7>
- Eliasson, A. C. (1983). Differential scanning calorimetry studies on wheat starch—gluten mixtures: I. Effect of gluten on the gelatinization of wheat starch. *Journal of Cereal Science*, 1(3), 199–205. [https://doi.org/10.1016/S0733-5210\(83\)80021-6](https://doi.org/10.1016/S0733-5210(83)80021-6)
- Fernández-Quintela, A., Macarulla, M. T., del Barrio, A. S., & Martínez, J. A. (1997). Composition and functional properties of protein isolates obtained from commercial legumes grown in northern Spain. *Plant Foods for Human Nutrition*, 51(4), 331–341. <https://doi.org/10.1023/A:1007936930354>
- Fonslick, J., & Khan, A. (1989). Thermal stability and composition of the amylose-iodine complex. *Journal of Polymer Science*, 27, 4161–4167.
- Garbow, J. R., & Schaefer, J. (1991). Magic-angle 13c nmr study of wheat flours and doughs. *Journal of Agricultural and Food Chemistry*, 39(5), 877–880. <https://doi.org/10.1021/jf00005a013>
- Gui, Y., Zou, F., Zhu, Y., Li, J., Wang, N., Guo, L., et al. (2022). The structural, thermal, pasting and gel properties of the mixtures of enzyme-treated potato protein and potato starch. *LWT*, 154, Article 112882. <https://doi.org/10.1016/j.lwt.2021.112882>
- Holló, J., & Szejtli, J. (1958). The mechanism of starch-iodine reaction. *Periodica Polytechnica, Chemical Engineering*, 2(1), 25–37.
- Hoover, R., Hughes, T., Chung, H. J., & Liu, Q. (2010). Composition, molecular structure, properties, and modification of pulse starches: A review. *Food Research International*, 43(2), 399–413. <https://doi.org/10.1016/j.foodres.2009.09.001>
- Huber, K. C., & Bemiller, J. N. (2017). 3.3.6.8 starch complexes. In S. Damodaran, & K. L. Parkin (Eds.), *Fennema's food chemistry* (5th ed., pp. 140–141). CRC Press.
- Johansson, M., Johansson, D., Ström, A., Rydén, J., Nilsson, K., Karlsson, J., et al. (2022). Effect of starch and fibre on faba bean protein gel characteristics. *Food Hydrocolloids*, 131, Article 107741. <https://doi.org/10.1016/j.foodhyd.2022.107741>
- Johansson, M., Nilsson, K., Knab, F., & Langton, M. (2022). Faba bean fractions for 3D printing of protein-, starch- and fibre-rich foods. *Processes*, 10(3). <https://doi.org/10.3390/pr10030466>
- Joshi, M., Aldred, P., Panozzo, J. F., Kasapis, S., & Adhikari, B. (2014). Rheological and microstructural characteristics of lentil starch–lentil protein composite pastes and gels. *Food Hydrocolloids*, 35, 226–237. <https://doi.org/10.1016/j.foodhyd.2013.05.016>
- Kimura, A., Fukuda, T., Zhang, M., Motoyama, S., Maruyama, N., & Utsumi, S. (2008). Comparison of physicochemical properties of 7S and 11S globulins from pea, faba bean, cowpea, and French bean with those of soybean—French bean 7S globulin

- exhibits excellent properties. *Journal of Agricultural and Food Chemistry*, 56(21), 10273–10279. <https://doi.org/10.1021/jf801721b>
- Kim, W., Wang, Y., & Selomulya, C. (2020). Dairy and plant proteins as natural food emulsifiers. *Trends in Food Science & Technology*, 105, 261–272. <https://doi.org/10.1016/j.tifs.2020.09.012>
- Langton, M., Ehsanzamir, S., Karkehabadi, S., Feng, X., Johansson, M., & Johansson, D. P. (2020). Gelation of faba bean proteins - effect of extraction method, pH and NaCl. *Food Hydrocolloids*, 103, Article 105622. <https://doi.org/10.1016/j.foodhyd.2019.105622>
- Langton, M., & Hermansson, A.-M. (1992). Fine-stranded and particulate gels of β -lactoglobulin and whey protein at varying pH. *Food Hydrocolloids*, 5(6), 523–539. [https://doi.org/10.1016/S0268-005X\(09\)80122-7](https://doi.org/10.1016/S0268-005X(09)80122-7)
- Larrea-Wachtendorff, D., Del Grosso, V., & Ferrari, G. (2022). Evaluation of the physical stability of starch-based hydrogels produced by high-pressure processing (HPP). *Gels*, 8(3), 152. <https://doi.org/10.3390/gels8030152>
- Larsen, F. H., Blennow, A., & Engelsen, S. B. (2008). Starch granule hydration-A MAS NMR investigation. *Food Biophysics*, 3(1), 25–32. <https://doi.org/10.1007/s11483-007-9045-4>
- Larsen, F. H., Kasprzak, M. M., Larke, H. N., Knudsen, K. E. B., Pedersen, S., Jørgensen, A. S., et al. (2013). Hydration properties and phosphorous speciation in native, gelatinized and enzymatically modified potato starch analyzed by solid-state MAS NMR. *Carbohydrate Polymers*, 97(2), 502–511. <https://doi.org/10.1016/j.carbpol.2013.05.014>
- Li, L., Yuan, T. Z., Setia, R., Raja, R. B., Zhang, B., & Ai, Y. (2019). Characteristics of pea, lentil and faba bean starches isolated from air-classified flours in comparison with commercial starches. *Food Chemistry*, 276(October 2018), 599–607. <https://doi.org/10.1016/j.foodchem.2018.10.064>
- Ma, K. K., Greis, M., Lu, J., Nolden, A. A., McClements, D. J., & Kinchla, A. J. (2022). Functional performance of plant proteins. *Foods*, 11(4), 594. <https://doi.org/10.3390/foods11040594>
- Morgan, K. R., Furneaux, R. H., & Larsen, N. G. (1995). Solid-state NMR studies on the structure of starch granules. *Carbohydrate Research*, 276(2), 387–399. [https://doi.org/10.1016/0008-6215\(95\)00173-Q](https://doi.org/10.1016/0008-6215(95)00173-Q)
- Muhrbeck, P., & Eliasson, A. (1991). Rheological properties of protein/starch mixed gels. *Journal of Texture Studies*, 22(3), 317–332.
- Multari, S., Stewart, D., & Russell, W. R. (2015). Potential of faba bean as future protein supply to partially replace meat intake in the human diet. *Comprehensive Reviews in Food Science and Food Safety*, 14(5), 511–522. <https://doi.org/10.1111/1541-4337.12146>
- Munialo, C. D., van der Linden, E., & de Jongh, H. H. J. (2014). The ability to store energy in pea protein gels is set by network dimensions smaller than 50nm. *Food Research International*, 64, 482–491. <https://doi.org/10.1016/j.foodres.2014.07.038>
- Nicolai, T., & Chassenieux, C. (2019). Heat-induced gelation of plant globulins. *Current Opinion in Food Science*, 27, 18–22. <https://doi.org/10.1016/j.cofs.2019.04.005>
- Nilsson, K., Sandström, C., Özeren, H. D., Vilaplana, F., Hedenqvist, M., & Langton, M. (2022). Physicochemical and thermal characterisation of faba bean starch. *Journal of Food Measurement and Characterization*, 16(6), 4470–4485. <https://doi.org/10.1007/s11694-022-01543-7>
- Núñez-Santiago, M. C., Bello-Pérez, L. A., & Tecante, A. (2004). Swelling-solubility characteristics, granule size distribution and rheological behavior of banana (*Musa paradisica*) starch. *Carbohydrate Polymers*, 56(1), 65–75. <https://doi.org/10.1016/j.carbpol.2003.12.003>
- Oñate Narciso, J., & Brennan, C. (2018). Whey and pea protein fortification of rice starches: Effects on protein and starch digestibility and starch pasting properties. *Starch/Stärke*, 70(9–10), 1–6. <https://doi.org/10.1002/star.201700315>
- Onwulata, C. I., Tunick, M. H., & Thomas-Gahring, A. E. (2014). Pasting and extrusion properties of mixed carbohydrate and whey protein isolate matrices. *Journal of Food Processing and Preservation*, 38(4), 1577–1591. <https://doi.org/10.1111/jfpp.12118>
- Punia, S., Dhull, S. B., Sandhu, K. S., & Kaur, M. (2019). Faba bean (*Vicia faba*) starch: Structure, properties, and in vitro digestibility—a review. *Legume Science*, 1(1), 3–7. <https://doi.org/10.1002/leg3.18>
- Ribotta, P. D., Colombo, A., León, A. E., & Añón, M. C. (2007). Effects of soy protein on physical and rheological properties of wheat starch. *Starch - Stärke*, 59(12), 614–623. <https://doi.org/10.1002/star.200700650>
- Richardson, G., Kidman, S., Langton, M., & Hermansson, A. M. (2004). Differences in amylose aggregation and starch gel formation with emulsifiers. *Carbohydrate Polymers*, 58(1), 7–13. <https://doi.org/10.1016/j.carbpol.2004.06.013>
- Richardson, G., Sun, Y., Langton, M., & Hermansson, A. M. (2004). Effects of Ca- and Na-lignosulfonate on starch gelatinization and network formation. *Carbohydrate Polymers*, 57(4), 369–377. <https://doi.org/10.1016/j.carbpol.2004.04.023>
- Röös, E., Carlsson, G., Ferawati, F., Hefni, M., Stephan, A., Tidåker, P., et al. (2020). Less meat, more legumes: Prospects and challenges in the transition toward sustainable diets in Sweden. *Renewable Agriculture and Food Systems*, 35(2), 192–205. <https://doi.org/10.1017/S1742170518000443>
- Sasaki, T., & Matsuki, J. (1998). Effect of wheat starch structure on swelling power. *Cereal Chemistry*, 75(4), 525–529. <https://doi.org/10.1094/CCHEM.1998.75.4.525>
- Schorsch, C., Wilkins, D. K., Jones, M. G., & Norton, I. T. (2001). Gelation of casein-whey mixtures: Effects of heating whey proteins alone or in the presence of casein micelles. *Journal of Dairy Research*, 68(3), 471–481. <https://doi.org/10.1017/S0022029901004915>
- Sharan, S., Zanghelini, G., Zotzel, J., Bonerz, D., Aschoff, J., Saint-Eve, A., et al. (2021). Fava bean (*Vicia faba* L.) for food applications: From seed to ingredient processing and its effect on functional properties, antinutritional factors, flavor, and color. *Comprehensive Reviews in Food Science and Food Safety*, 20(1), 401–428. <https://doi.org/10.1111/1541-4337.12687>
- Shim, J., & Mulvaney, S. J. (2001). Effect of heating temperature, pH, concentration and starch/whey protein ratio on the viscoelastic properties of corn starch/whey protein mixed gels. *Journal of the Science of Food and Agriculture*, 81(8), 706–717. <https://doi.org/10.1002/jsfa.869>
- Tanger, C., Müller, M., Andlinger, D., & Kulozik, U. (2022). Influence of pH and ionic strength on the thermal gelation behaviour of pea protein. *Food Hydrocolloids*, 123, Article 106903. <https://doi.org/10.1016/j.foodhyd.2021.106903>
- Tang, H., & Hills, B. P. (2003). Use of ¹³C MAS NMR to study domain structure and dynamics of polysaccharides in the native starch granules. *Biomacromolecules*, 4(5), 1269–1276.
- Tester, R. F., & Morrison, W. R. (1990). Swelling and gelatinisation of cereal starches I. Effect of amylopectin, amylose and lipids. *Cereal Chemistry*, 65(6), 551–557.
- Vamadevan, V., & Bertoff, E. (2020). Observations on the impact of amylopectin and amylose structure on the swelling of starch granules. *Food Hydrocolloids*, 103, Article 105663. <https://doi.org/10.1016/j.foodhyd.2020.105663>
- Vogelsang-O'Dwyer, M., Petersen, I. L., Joehne, M. S., Sørensen, J. C., Bez, J., Detzel, A., et al. (2020). Comparison of faba bean protein ingredients produced using dry fractionation and isoelectric precipitation: Techno-functional, nutritional and environmental performance. *Foods*, 9(3), 322. <https://doi.org/10.3390/foods9030322>
- Walstra, P. (2002). Physical chemistry of foods. In O. R. Fennema, Y. H. Hui, M. K. Rutgers, P. Walstra, & J. R. Whitaker (Eds.), *Physical chemistry of foods*. Marcel Dekker Inc. <https://doi.org/10.1201/9780203910436>
- Warsame, A. O., O'Sullivan, D. M., & Tosi, P. (2018). Seed storage proteins of faba bean (*Vicia faba* L.): Current status and prospects for genetic improvement. *Journal of Agricultural and Food Chemistry*, 66(48), 12617–12626. <https://doi.org/10.1021/acs.jafc.8b04992>
- Willett, W., Rockström, J., Loken, B., Springmann, M., Lang, T., Vermeulen, S., et al. (2019). Food in the anthropocene: The EAT–lancet commission on healthy diets from sustainable food systems. *The Lancet*, 393(10170), 447–492. [https://doi.org/10.1016/S0140-6736\(18\)31788-4](https://doi.org/10.1016/S0140-6736(18)31788-4)
- Winter, H. H., & Chambon, F. (1986). Analysis of linear viscoelasticity of a crosslinking polymer at the gel point. *Journal of Rheology*, 30(2), 367–382. <https://doi.org/10.1122/1.549853>
- Yang, H., Irudayaraj, J., Otgonchimeg, S., & Walsh, M. (2004). Rheological study of starch and dairy ingredient-based food systems. *Food Chemistry*, 86(4), 571–578. <https://doi.org/10.1016/j.foodchem.2003.10.004>
- Yang, N., Liu, Y., Ashton, J., Gorkczyca, E., & Kasapis, S. (2013). Phase behaviour and in vitro hydrolysis of wheat starch in mixture with whey protein. *Food Chemistry*, 137(1), 76–82. <https://doi.org/10.1016/j.foodchem.2012.10.004>
- Yang, C., Zhong, F., Goff, H. D., & Li, Y. (2019). Study on starch-protein interactions and their effects on physicochemical and digestible properties of the blends. *Food Chemistry*, 280, 51–58. <https://doi.org/10.1016/j.foodchem.2018.12.028>
- Zhang, D., Mu, T., & Sun, H. (2017). Calorimetric, rheological, and structural properties of potato protein and potato starch composites and gels. *Starch - Stärke*, 69(7–8), Article 1600329. <https://doi.org/10.1002/star.201600329>
- Zhang, B., Qiao, D., Zhao, S., Lin, Q., Wang, J., & Xie, F. (2021). Starch-based food matrices containing protein: Recent understanding of morphology, structure, and properties. *Trends in Food Science & Technology*, 114, 212–231. <https://doi.org/10.1016/j.tifs.2021.05.033>
- Zhang, Z., Tian, X., Wang, P., Jiang, H., & Li, W. (2019). Compositional, morphological, and physicochemical properties of starches from red adzuki bean, chickpea, faba bean, and baiyue bean grown in China. *Food Sciences and Nutrition*, 7(8), 2485–2494. <https://doi.org/10.1002/fsn3.865>
- Zha, F., Rao, J., & Chen, B. (2021). Plant-based food hydrogels: Constitutive characteristics, formation, and modulation. *Current Opinion in Colloid & Interface Science*, 56, Article 101505. <https://doi.org/10.1016/j.cocis.2021.101505>
- Zhu, F. (2017). NMR spectroscopy of starch systems. *Food Hydrocolloids*, 63, 611–624. <https://doi.org/10.1016/j.foodhyd.2016.10.015>